

ISTANBUL TECHNICAL UNIVERSITY ★ GRADUATE SCHOOL OF SCIENCE
ENGINEERING AND TECHNOLOGY

**WELL TESTING FOR HEAVY OIL
SAGD OPERATIONS**

M.Sc. THESIS

Elnaz GHAFOURI AIAN

Department of Petroleum and Natural Gas Engineering

Petroleum and Natural Gas Engineering Programme

Thesis Advisor: Prof. Dr. Abdurrahman SATMAN

APRIL 2015

ISTANBUL TECHNICAL UNIVERSITY ★ GRADUATE SCHOOL OF SCIENCE
ENGINEERING AND TECHNOLOGY

**WELL TESTING FOR HEAVY OIL
SAGD OPERATIONS**

M.Sc. THESIS

**Elnaz GHAFOURI AIAN
(505101514)**

Department of Petroleum and Natural Gas Engineering

Petroleum and Natural Gas Engineering Programme

Thesis Advisor: Prof. Dr. Abdurrahman SATMAN

APRIL 2015

İSTANBUL TEKNİK ÜNİVERSİTESİ ★ FEN BİLİMLERİ ENSTİTÜSÜ

**AĞIR PETROL SAHALARINDA SAGD UYGULAMALARINDA KUYU
TESTLERİ**

YÜKSEK LİSANS TEZİ

**Elnaz GHAFOURI AIAN
(505101514)**

Petrol ve Doğal Gaz Mühendisliği Anabilim Dalı

Petrol ve Doğal Gaz Mühendisliği Programı

Tez Danışmanı: Prof. Dr. Abdurrahman SATMAN

2015 NISAN

Elnazghafouri Aian, a **M.Sc.** student of **ITU Graduate School of Science, Engineering and Technology** student ID 505101514, successfully defended the thesis entitled “**WELL TESTING FOR HEAVY OIL SAGD OPERATIONS**”, which she prepared after fulfilling the requirements specified in the associated legislations, before the jury whose signatures are below.

Thesis Advisor : **Prof. Dr.Abdurrahman SATMAN**
Istanbul Technical University

Jury Members : **Prof. Dr. Sabri Erkin NASUF**
Istanbul Technical University

Doç.Dr. Ömer İnanç TÜREYEN
Istanbul Technical University

Date of Submission : 21 April 2015
Date of Defense : 25 May 2015

FOREWORD

This master thesis has been prepared for the degree Master of Science in Petroleum and Natural Gas Engineering at Istanbul Technical University, under the supervision of Professor **Abdurrahman Satman**, during summer 2013 to spring 2015. I want to express my sincere gratitude to my supervisor Professor Satman for encouragement, guidance and kindly helping and supporting me during this work and I am thankful to Doç.Dr Murat Çinar for answering my questions related to STARS and SAGD process. Finally I would like to express infinite gratitude to my parents, my twin sister Sanaz and my best friend Peyman for perpetual support during all education years.

April 2015

Elnaz GHAFOURI AIAN

TABLE OF CONTENTS

| | <u>Page</u> |
|--|-------------|
| FOREWORD | vii |
| TABLE OF CONTENTS | ix |
| ABBREVIATIONS | xi |
| LIST OF TABLES | xiii |
| LIST OF FIGURES | xv |
| SUMMARY | xvii |
| ÖZET | xix |
| 1. INTRODUCTION | 1 |
| 1.1 Literature Review | 2 |
| 1.1.1 Heavy oil | 2 |
| 1.1.2 World oil sand reserves and Athabasca oil reservoir | 4 |
| 1.2 Purpose of Thesis | 6 |
| 2. PRODUCTION TECHNIQUE AND RECOVERY OF OIL SANDS | 7 |
| 2.1 Recovery of Oil Sands | 7 |
| 2.2 The Steam Assisted Gravity Drainage (SAGD) Mechanism | 8 |
| 2.2.1 SAGD mechanism | 11 |
| 2.2.2 SAGD design issues | 12 |
| 2.2.2.1 Well spacing | 13 |
| 2.2.2.2 Implications of thief zone | 13 |
| 2.2.3 Criteria for evaluating performance | 14 |
| 2.3 Horizontal Well | 15 |
| 2.3.1 Horizontal injection wells | 16 |
| 2.3.2 Vertical injection wells | 17 |
| 3. THERMAL WELL TESTING | 19 |
| 3.1 Viscosity and Temperature | 19 |
| 3.2 Steamflood Front Mechanism | 21 |
| 3.3 Relative Permeability | 24 |
| 3.4 Transient Well Test | 25 |
| 3.5 Method of Analysis | 26 |
| 3.6 Reservoir Simulation Model | 28 |
| 3.6.1 Methodology for estimating swept volume from falloff test data. | 30 |
| 3.6.2 Estimating swept volume from numerical simulation. | 36 |
| 4. DISCUSSION OF RESULTS | 37 |
| 4.1 Results from Simulator | 37 |
| 4.2 Results from Calculation by Using PSS Method | 39 |
| 4.3 Effect of Injection Time, Injection Rate and Steam Injection Quality on Pressure Behavior | 40 |
| 4.3.1 Effect of injection time on steam chamber estimation | 40 |
| 4.3.2 Effect of injection rate on steam chamber estimation | 44 |
| 4.3.3 Effect of injection quality on steam chamber estimation | 44 |

| | |
|------------------------------|-----------|
| 5. CONCLUSIONS | 47 |
| REFERENCES..... | 49 |
| APPENDICES | 53 |
| APPENDIX A.1 | 54 |
| APPENDIX A.2 | 57 |
| CURRICULUM VITAE..... | 59 |

ABBREVIATIONS

| | |
|----------------|---|
| API | : American Petroleum Institute |
| BTU | : British Thermal Unit |
| CMG | : Computer Modeling Group |
| CSOR | : Cumulative Steam Oil Ratio |
| CSS | : Cyclic Steam Stimulation |
| CWE | : Cold Water Equivalent |
| EOR | : Enhanced Oil Recovery |
| ETR | : Early Time Region |
| LTR | : Late Time Region |
| MDH | : Miller-Dye-Hutchinson |
| MTR | : Middle Time Region |
| PBU | : Pressure Buildup |
| PFO | : Pressure Falloff |
| PSS | : Pseudo Steady State |
| SAGD | : Steam Assisted Gravity Drainage |
| SOR | : Steam Oil Ratio |
| STARS | : Steam, Thermal and Advanced Processes Reservoir Simulator |
| STB/day | : Stock Tank Barrel per day |
| 3D | : Three Dimensional |

LIST OF TABLES

| | <u>Page</u> |
|--|-------------|
| Table 3.1 : Reservoir and fluid parameters for vertiac l well..... | 30 |
| Table 3.2 : Grid block sizes..... | 30 |
| Table 4.1 : Average values of temperature, gas saturation, water saturation and gas phase mobility. | 37 |
| Table 4.2 : Results of the simulated falloff tests and conditions..... | 46 |
| Table A.1: Average values of temperature, gas saturation, water saturation and gas phase mobility for various steam injection times. | 54 |
| Table A.2: Average values of temperature, gas saturation, water saturation and gas phase mobility for various steam injection rates..... | 55 |
| Table A.3: Average values of temperature, gas saturation, water saturation and gas phase mobility for various steam injection qualities..... | 56 |

LIST OF FIGURES

| | <u>Page</u> |
|--|-------------|
| Figure 1.1 : Thermal recovery-SAGD method | 2 |
| Figure 1.2 : Definition of heavy oil and bitumen..... | 3 |
| Figure 1.3 : Composition of oil sands. | 3 |
| Figure 1.4 : Comparison of world proven oil reserves with Canada. | 4 |
| Figure 1.5 : Major oil sand deposits of Canada. | 5 |
| Figure 2.1 : The extraction techniques employed in oil sands recovery..... | 7 |
| Figure 2.2 : Cross-sectional view of the CSS concept..... | 8 |
| Figure 2.3 : Cross-sectional view of the SAGD concept. | 9 |
| Figure 2.4 : Basic description of SAGD process.. | 12 |
| Figure 2.5 : SAGD start-up time versus spacing. | 14 |
| Figure 2.6 : Growth of steam chamber with horizontal producer and injector | 17 |
| Figure 2.7 : Growth of steam chamber with horizontal producer and vertical injector. | 17 |
| Figure 3.1 : Viscosity of Athabasca bitumen versus temperature..... | 20 |
| Figure 3.2 : Temperature profile in the reservoirs and around the injector. | 22 |
| Figure 3.3 : Steamflooding advance. | 22 |
| Figure 3.4 : Water/oil relative permeability curve..... | 25 |
| Figure 3.5 : Gas/oil relative permeability curve. | 25 |
| Figure 3.6 : Falloff test..... | 27 |
| Figure 3.7 : Specific flow regimes within all categories in fall-off test..... | 28 |
| Figure 3.8 : 3D view of well configuration in the numerical simulation model..... | 29 |
| Figure 3.9 : 3D view of displaying open intervals of the injection well..... | 29 |
| Figure 3.10 : Logarithmic pressure derivative data for 1 day shut-in time after 50 days injection. | 31 |
| Figure 3.11 : Cartesian pressure data for 1 day shut-in after 50 days injection..... | 32 |
| Figure 3.12 : Appearance of Cartesian straight line for 1day shut-in after 50 days injection | 32 |
| Figure 3.13 : Semilog pressure data for 1 day shut-in after 50 days injection..... | 35 |
| Figure 3.14 : Appearance of semilog straight line for 1day shut-in after 50 days injection. | 35 |
| Figure 4.1 : 50 days steam injection: (a) Temperature, (b) Water saturation, (c) Gas phase mobility, (d) Gas saturation | 38 |
| Figure 4.2 : Steam injection times: (a) 20 days, (b) 30 days, (c) 40 days, (d) 50 days. | 41 |
| Figure 4.3 : Swept volume changes versus injection times. | 42 |
| Figure 4.4 : Bottom hole pressures versus various injection times.. | 42 |
| Figure 4.5 : Log-log diagnostic plot of bottom hole shut-in pressure versus shut-in time for various injection time... .. | 43 |
| Figure 4.6 : Cartesian plot of bottom hole shut-in pressure versus shut-in time for various injection times.... .. | 43 |

| | |
|---|----|
| Figure 4.7 : Semilog plot of bottom hole shut-in pressure versus shut-in time for various injection time..... | 44 |
| Figure 4.8 : Swept volume changes versus injection times. ... | 45 |
| Figure 4.9 : Swept volume changes versus steam injection qualities. ... | 45 |
| Figure A.1 : Steam injection rates: (a) 200 STB/day, (b) 500 STB/day, (c) 1000 STB/day, (d) 1500 STB/day..... | 57 |
| Figure A.2 : Steam injection qualities: (a) 60%, (b) 70%, (c) 80%..... | 58 |

WELL TESTING FOR HEAVY OIL SAGD OPERATIONS

SUMMARY

Thermal Recovery is one of the common EOR recovery methods. Thermal recovery methods are used worldwide to recover heavy oil and bitumen. Thin layer of water between the quartz and the bitumen makes the oil sands water-wet, this plays an important role in the separation of bitumen from the quartz by use of a hot-water extraction technique.

High oil prices are pushing the application of horizontal wells in thermal recovery methods. The possibility of horizontal drilling has created a pathway for SAGD (Steam Assisted Gravity Drainage), which is the most preferred heavy oil and bitumen recovery method.

Oil recovery by steam injection requires knowledge of the steam-swept pore volume. The determination of the swept volume in a thermal oil recovery process makes it possible to do early economic evaluation; it means rapid measurement of the fuel concentration for an in-situ combustion operation, and the heat loss from a steam zone.

In field operations, the swept volume has been determined by coring and/or temperature observations made at wells during passage of the displacement front. Well testing evaluates the steam-swept volume by inexpensive and a relatively quick way. The aim of the thesis will be to estimate swept volume and steam chamber mobility by using pressure falloff tests of vertical well.

Satman, Eggenschwiler and Ramey (1980) presented a method to estimate the steam zone mobility and swept volume using pressure falloff test; assuming two regions of highly contrasting fluid mobility and an impermeable boundary interface in a composite reservoir. Consequently, for a short duration, the swept zone acts as a closed reservoir, during which the pressure response shows the pseudo steady state behavior.

Falloff tests are simulated by shutting-in the injector and recording the wellbore pressure with time. The MDH (Miller-Dyes-Hutchinson) method for the analysis of falloff data is used because the shut-in time is much less than the injection time in practical steam injection falloff tests. The pseudosteady state (PSS) method is used to estimate the swept volume, from pressure fall off testing of vertical wells.

A homogeneous square box reservoir, in CMG (STARS) simulator, is used to model steam chamber profile. Injection rate, injection time, steam injection quality and gas (steam) mobility relations with time are investigated by using simulator and comparison with PSS method. The simulation and application of case model is described and finally, comprehensive discussion of the analyses, results and conclusions are given. The results obtained in this study yields reliable results when the swept volume is sufficiently large, so that a proper Cartesian straight line behavior exist.

AĞIR PETROL SAHALARINDA SAGD UYGULAMALARINDA KUYU TESTLERİ

ÖZET

Küresel ham petrol fiyatlarının yükselmesi nedeniyle petrol kumları gibi alışlagelmemiş ağır petrolerin üretilmesi oldukça kârlı bir düzeye erişmiştir. Venezuela, Kanada ve Suudi Arabistan petrol kaynak rezervi olarak dünyada ilk üç ülke olarak sıralanmaktadır. Kanada'nın 174 milyar varil olan ham petrol rezervinin %97'si sadece Alberta Eyaleti petrol kumlarıdır.

Isıl üretim arttırma yöntemi petrol üretim arttırma yöntemlerinden birisidir. Dünyada ağır petroler ve bitümen gibi oldukça ağır petroleri üretmek için en çok kullanılan yöntem, ısıl üretim arttırma yöntemidir. Isıl üretim arttırma yöntemleri; yerinde yakma, sürekli buhar, ve çevrimsel buhar yöntemleri olarak sınıflandırılmaktadır.

Kanada Alberta Eyaleti petrol kumlarını ısıl üretim arttırma yöntemi olarak buhar destekli yerçekimi drenajı (SAGD) yöntemiyle üretmektedir.

SAGD yöntemi, petrol kumları yatağı içerisinde beş metre aralıklı iki yatay kuyu (enjeksiyon kuyusu üretim kuyusunun üstünde) olarak uygulanmaktadır. SAGD yönteminde, buhar enjeksiyonu yöntemi kullanıldığında, 570 °F'dan yüksek sıcaklıklı ve yüksek basınçlı buhar, yaklaşık 1000-1500 ft derinliklerindeki enjeksiyon kuyusuna basılmakta, ağır petrolü ısıtmakta ve sıvılaşmasına neden olmaktadır.

SAGD yöntemi; yatay kuyu kullanılarak rezervuarın buharla çok büyük alanda temasta olması sağlandığından dolayı tercih edilmektedir. Buhar basma ile petrol üretiminde, buharla dolu zonun hacmini bilmek uygulamaların verimliliğini incelerken önemlidir.

Bu araştırmada ısıl üretim arttırma yöntemlerinden buhar destekli yerçekimi drenajı (SAGD) yöntemi incelenmiştir. Öncelikle buhar destekli yerçekimi drenajı prosesi ve üretim mekanizmaları göz önünde bulundurulmakta, daha sonra bu yöntem uygulanırken yapılan kuyu testleri konusu incelenmektedir. Çeşitli mühendislik parametreleri; farklı yönlerde rezervuar geçirgenliği (anisotropy) , zar faktörü (skin factor), gözeneklilik (porosity), v.b., parametreler ve etkileri incelenmektedir.

Modellemede iki farklı grid yaklaşımı kullanılarak, buhar enjeksiyonu süresi, su buharı enjeksiyon debileri ve farklı kalitelerde buhar basma dikkate alınarak senaryolar oluşturulmuştur. Bu senaryolar için kuyu dibi basıncının zamanla değişimi gözlemlendi ve kuyu testlerinde kullanıldı.

Bu tez araştırması Computer Modeling Group (CMG) STARS 2012.12 simulator programı kullanılarak gerçekleştirilmiştir. Rezervuar simülasyonunda 3D modeli oluşturuldu ve rezervuar ve akışkan özellikleri veri olarak modele girildi. Simülasyon modelinde sadece düşey enjeksiyon kuyusu incelendi. Bu enjeksiyon kuyu konumu için yukarıda bahsedilen parametreleri dikkate alarak, simülasyondan elde edilen ve Satman et al. (1980) yöntemi ile en iyi hangisinin uyuşduğunu göz altına alındı.

Kuyu testleri analizinde genellikle basınç yükselme dönemine ait basınç ve basınç-türev sinyalleri analiz edilir. İncelenen yöntemde (SAGD) enjeksiyon/basınç düşüm ("injection/falloff") testi, tek kuyu kullanımı ile yapılan testlerdir ve genellikle testlerde kapama zamanında ölçülen basınçların analizi daha güvenilir sonuçlar vermektedir. Bu testin analizi ile enjeksiyon kuyularının verimliliği ve enjekte edilen buharın rezervuar içerisindeki yayılımı (cephesi) belirlenmektedir.

Kuyu basınç testleri analizinde, kuyu geometrisine, rezervuar yapısına ve sınır koşullarına, akış ve akışkan türüne bağlı olarak kullanılabilecek pek çok model mevcuttur ama bu araştırmada MDH (Miller-Dyes-Hutchinson) kuyu testlerinin yöntemi, temel ilkeleri, test tipleri ve analizleri hakkında bilgiler verildi ve kullanıldı. Basınç-zaman veya basınç-türevi-zaman verileri, log-log, yarılog ve kartezyen grafiklerde çizilir ve analiz yaparken, kuyu içi depolama, çevrel akış, doğrusal akış, küresel akış, vs. akış rejimleri tanımlanır. Rezervuar-kuyu sisteminin basınç üzerinde meydana getirdiği değişimlerin türev eğrisinde, basınç-türev fonksiyonu kullanılır. Bu nedenle, kuyu basınç testleri analizinde, basınca ek olarak basınç-türev eğrilerinin kullanımı standart bir araç olmuştur. Basınç-türev fonksiyonu, kaydedilmiş kuyu dibi basıncının (veya sabit bir basınç değeri; basınç azalım testlerinde ilk basınç, basınç yükselme testlerinde ise kapama anındaki kuyu dibi akış basıncı, referans alınarak oluşturulan basınç değişiminin) zamanın doğal logaritmasına göre türevi olarak tanımlanır. Basıncın zamanın logaritmasına göre türev alınmasının iki temel nedeni vardır. Birincisi doğal logaritmaya göre türev alındığında, basınç-türev fonksiyonun fiziksel birimi basıncın birimiyle (örneğin psi, bar, vs) ile aynı olur. İkincisi ise, kuyuya çevrel akışın ("radial flow") olduğu durumlarda, basınç (veya basınç değişimi) zamanın doğal logaritması ile değiştiğinden, bu akış rejimi döneminde basınç-türev eğrisi sabit bir değer alır.

Basınç-türev fonksiyonun test zamanı t' ye karşı log-log grafiğinde çevrel akış dönemi sıfır eğimli bir doğru ile tanınır. Erken zamanlarda gözlemlenen kuyu içi depolaması etkileri basınç/zaman ve basınç-türev/zaman log-log grafiklerinde +1 (birim) eğimli doğru ile tanınır. Geç zamanlarda kuyuya yakın beslenmeli bir sınır ya da fay kendini basınç-türev/zaman log-log grafiğinde +1 eğimli doğru ile gösterir.

Basınç düşüm testlerinde (falloff) Δt kapama anından itibaren ölçülen zamanı temsil eder.

Bu araştırmada 500 STB/day debide toplam 30 gün buhar enjeksiyonu yapılmakta ve 1 gün (24 saat) kapatılmaktadır. Δp basınç yükselme testlerinde kapama anındaki kuyu dibi akış basıncı ile kaydedilmiş kuyu dibi basıncının farkıdır.

Her akış ve kapama dönemine ait basınç-zaman verilerinin uygun şekilde analizi ile akışkan/kayaç/zar faktörü parametrelerine ait değerler belirlenebilir. Buhar zonunun hacimi, basınç-zaman grafiğinden elde edilen eğimden yararlanarak hesaplanabilir. Basınç-zaman yarılog eğimi ise etken geçirgenliğin hesaplamasında kullanılır. Zar faktörü basınç-zaman yarılog grafiğinin üzerinde 1 saat kapama zamanındaki basınç değerini okuyarak ve gerekli denklem kullanarak hesaplanabilir. Çeşitli su buharı enjeksiyon debileri, farklı kaliteli buharlar ve farklı enjeksiyon zamanı dikkate alınarak senaryolar oluşturulmuştur.

Buhar enjeksiyon süresi 20, 30, 40 ve 50 gün alınarak buhar zonunun hacmine ve mobilitesine etkisi incelendi. Buhar enjeksiyonun debisi 200, 500, 1000 ve 1500 STB/gün alındı ve buhar zonunun hacmine ve mobilitesine etkisi değiştiği incelendi. Enjekte edilen buharın kalitesi % 60, 70 ve 80 alınarak, buhar zonunun hacmine ve mobilitesine etkisi incelendi.

Bütün bu sonuçlar yarı kararlı akış yöntemi ile (PSS) karşılaştırıldı. Simulatörden elde edilen sonuçlarla kullandığımız yöntemin (Satman-Eggenschwiler-Ramey

yöntemi ile çok iyi uyduğu görülmüştür. Sadece kısa enjeksiyon zamanlarında ve düşük kaliteli buhar kullanıldığında sonuçlar arasında fark gözlemlendi. Bunun nedeni kısa enjeksiyon zamanlarında ve düşük kaliteli buhar kullandığımızda iyi bir buhar zonu oluşmadığı için, yarı kararlı akış davranış eğilimlerinin okumasında ki hatalar olarak düşünülmektedir.

1. INTRODUCTION

In this part, a review of some literature dealing with this thesis subject is given. Various types and sizes of heavy oil deposits are found in the world. Among them, Alberta (in Canada), Alaska (in the United States), and the Orinoco belt (in Venezuela) are the most explored and biggest reserves. The initial oil in place in Alberta is estimated to be 174 billion bbl, however it is expected that this number will increase as exploratory methods continue to develop.

Thermal recovery is one of the common EOR recovery methods. Thermal recovery methods are used worldwide to recover heavy oil and bitumen. The basic process concept involved in thermal recovery processes is to generate hot fluid on the surface or in situ and inject it through an injection well into an oil-bearing formation. The steam will heat the oil and displace it toward the producing well where it is pumped to the surface. High oil prices are pushing the application of horizontal wells in thermal recovery methods. The possibility of horizontal drilling has created a pathway for SAGD (Steam Assisted Gravity Drainage), which is the most preferred heavy oil and bitumen recovery method. Figure 1.1 illustrates a schematic view of a SAGD process. The mechanism of SAGD involves two parallel horizontal wells, with the production well situated at the bottom of the reservoir and the injection well placed above. Steam injected heats up the oil and oil viscosity decreases, so oil is able to flow to the production well by gravity drainage.

Oil recovery by steam injection requires knowledge of the steam-swept pore volume. The determination of the swept volume in a thermal oil recovery process makes the early economic evaluation; it means rapid measurement of the fuel concentration for an in-situ combustion operation, and the heat loss from a steam zone. In field operations, the swept volume has been determined by coring and/or temperature observations made at wells during passage of the displacement front.

Well testing evaluates the steam-swept volume by inexpensive and a relatively quick way. The pseudosteady state method has been used to estimate the swept volume,

from pressure fall off testing of vertical wells. However, horizontal well testing is more complex than vertical well testing, but the employment of horizontal wells instead of vertical wells helps to increase the oil production, because provides large contact area for the reservoir and also reduces gas and water coning problems, and also the drilling technology of horizontal wells is economical.

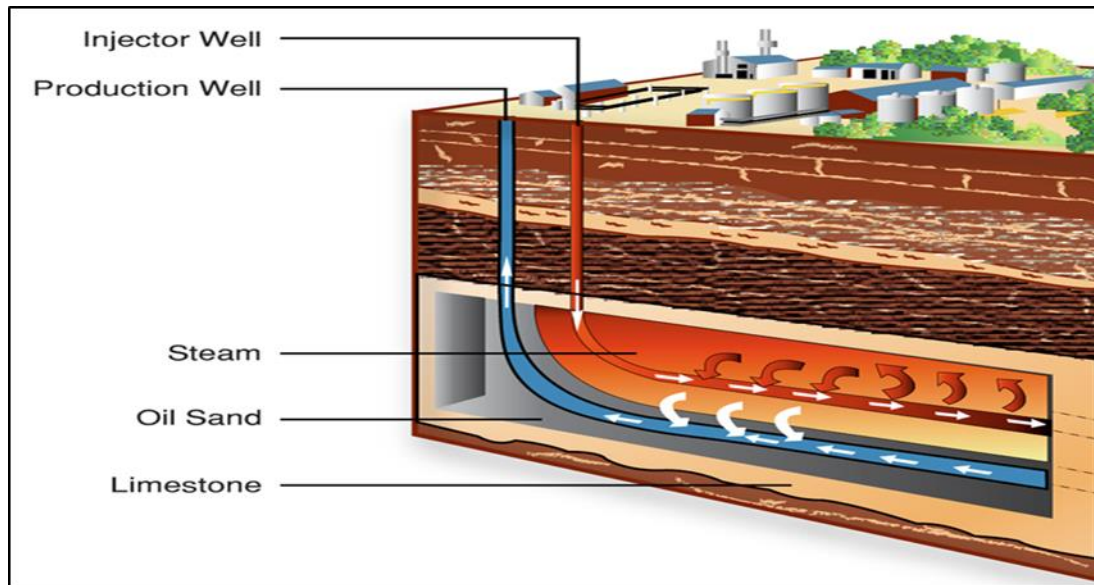


Figure 1.1 : Thermal recovery-SAGD method (Url-1)

1.1 Literature Review

1.1.1 Heavy oil

Definitions of heavy oil and bitumen are shown graphically in Figure 1.2. The value of 10 °API, which is equivalent to that of water, provides a clear border between unconventional, extra heavy oil and conventional heavy oil. However, it is more accurate to define heavy oil in terms of viscosity, rather than API gravity. Crude oil below 10 °API with viscosity of 1000–10000 cp is considered as extra heavy oil, and that with viscosity above 10000 cp is considered as bitumen.

Oil sands are a mixture of sand/clays, bitumen and water, also referred to as tar sands or bituminous sands as shown in Figure 1.3. Bitumen is the oil component of oil sands and sticky form of crude oil. It is so heavy, viscous and immobile at normal conditions. Its density range and viscosity are 8° to 12° API and 50000 cp,

respectively. Viscosity of bitumen at 200°C is close to water, which is enough to pump it, along with the produced water through the production well.

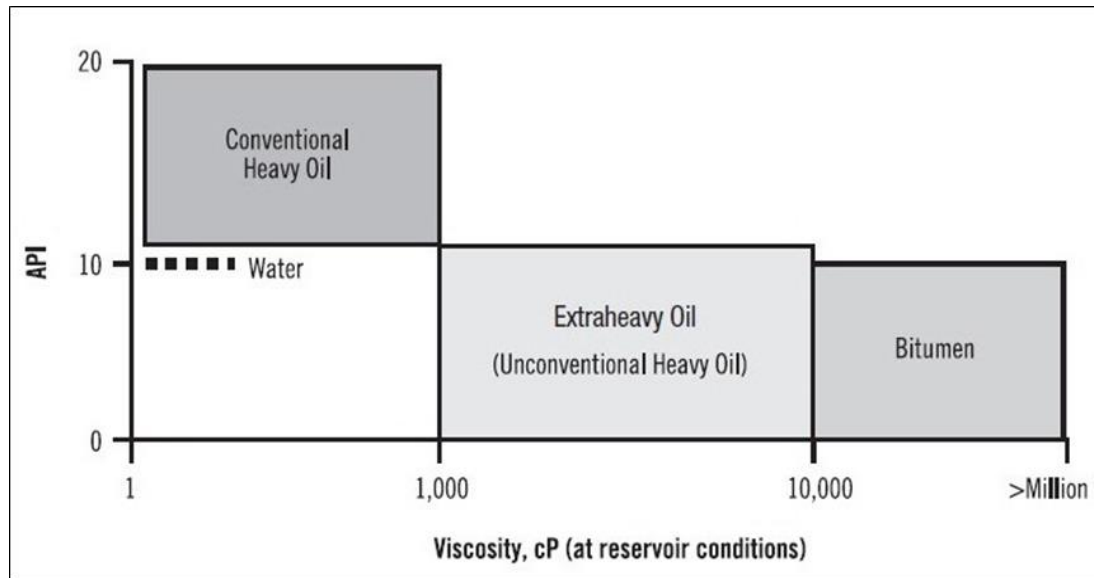


Figure 1.2 : Definition of heavy oil and bitumen (Banerjee, 2012).

Thin layer of water, around 10 microns across, between the quartz and the bitumen makes the oil sands water-wet, this plays an important role in the separation of bitumen from the quartz by use of a hot-water extraction technique. Bitumen is a complex mixture of hydrocarbons containing carbon, hydrogen, nitrogen, and sulfur (CHNS). Bitumen is a high-acid crude of average TAN value (total acid number) of 2.5 mg KOH/gram of sample.



Figure 1.3 : Composition of oil sands (Url-2).

The API° gravity is related to the conventional specific gravity γ_o by equation (1.1):

$$\text{API}^\circ \text{ gravity} = \frac{141.5}{\gamma_o} - 131.5 \quad (1.1)$$

1.1.2 World oil sand reserves and Athabasca oil reservoir

As shown in Figure 1.4 various sizes of heavy oil deposits are found in the world. Among them, those in Alberta (in Canada), Alaska (in the United States), and the Orinoco belt (in Venezuela) are the most explored and biggest reserves. The deposits in Alaska and the Orinoco belt, which by definition, fall into the extra heavy oil group.

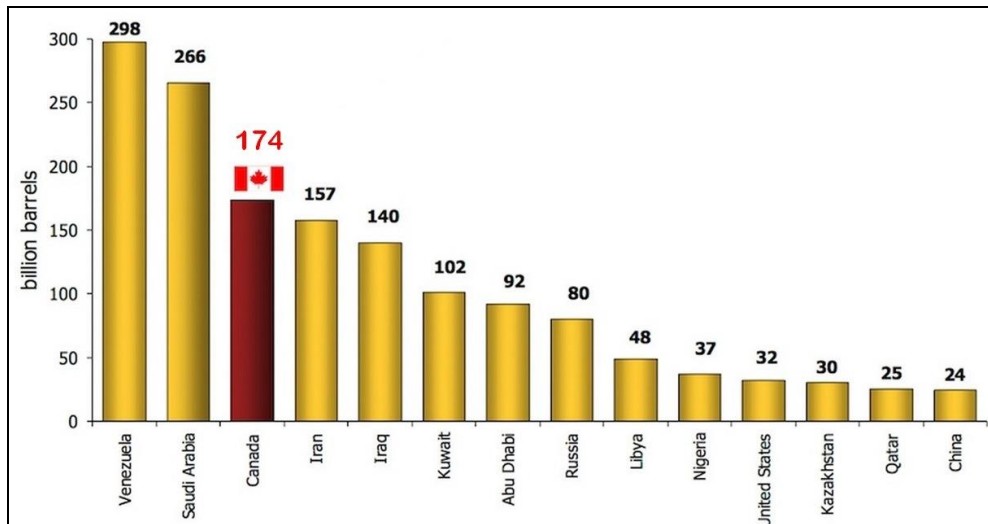


Figure 1.4 : Comparison of world proven oil reserves with Canada (Url-3).

Alberta's deposits are made of oil sands containing very highly viscous hydrocarbons that fall in the category of bitumen. Alberta's oil sands are early Cretaceous in age, which means that the sands that contain the bitumen were originally laid down about 100 million years ago. Recently, huge resources of heavy oil and bitumen have been discovered worldwide. According to Chen et al. (2008), the heavy oil in place in Venezuela is more than 1.8 trillion bbl, 1.7 trillion bbl in Alberta, Canada, and 20–25 billion bbl on the North Slope of Alaska.

As seen in Figure 1.5, there are major bitumen deposits in Alberta. Alberta has four main deposits. In the northeastern part, the largest one is Athabasca, and the second largest is Cold Lake, south of Athabasca. Two much smaller deposits are located on

the western part of the Athabasca area, Peace River. Most of the bitumen deposits, in the Athabasca oil sand, are found within Fort McMurray interval. Athabasca oil sands deposit is located in Northern Alberta and is the largest petroleum accumulation in the world, covering an area of about one trillion barrels of original bitumen-in-place. This amount comprises two-thirds of Alberta's total oil reserves and 20% of Canada's. According to the Canadian Association of Petroleum Producers, current oil sands production is about 1 million barrels of oil per day. Over half of Canada's crude oil production is from the oil sands. Production is estimated to reach almost 4 million barrels per day by 2020. Canadian heavy oil that is obtained from the oil sands or carbonates, has an API gravity less than 10° and a viscosity above 10000 cp at reservoir conditions, where the average reservoir temperature is 10–12°C (50–52°F) (Sheng, 2013).

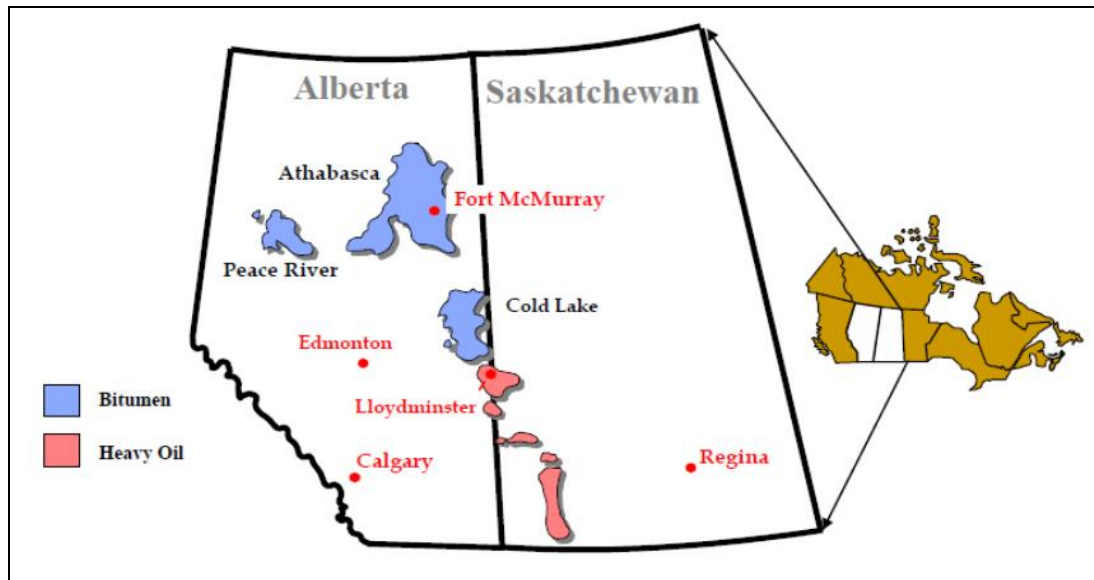


Figure 1.5 : Major oil sand deposits of Canada (Nasr et al., 2005).

Alberta oil sands have seen over 30 years of SAGD applications and numerous numerical and experimental studies have been conducted to evaluate the performance of SAGD process under different conditions. The field experience of SAGD process in UTF project in Alberta, Canada, was successful (Edmunds et al., 1994, and O'Rourke et al., 1994). There are many other SAGD processes being conducted in commercial stage in Alberta oil sands, (Butler et al., 2001). Recently, Laricina Energy planned to apply SAGD pilot project at Saleski, Grosmont, Alberta, Canada reservoir (Url-4). Cimolai et al. (2008), mentioned that SAGD is the best thermal process however, did not present the results of the simulation. Laricina Company

Operation Report (2010) started to apply SAGD (1800 barrels per day capacity) at Saleski, December 2010 as the world's first SAGD carbonate project and oil production was initiated in the spring of 2011 (Url-5).

1.2 Purpose of Thesis

Volume of heavy oil reserves are double in compared to conventional oil reserves. As conventional oil reservoirs are depleting, unconventional reservoirs play a good role in covering parts of the future energy demand. The papers published by Satman et al. (1980), Jahanbani et al. (2011), Shamila et al. (2005) and Tarhuni et al. (2004) are studied in detail in this thesis. Vertical wells configurations were simulated to compare with mentioned papers results and different configurations. The thermal simulator, CMG STARS (Computer Modeling Group; Steam, Thermal and Advanced Processes Reservoir Simulator) is employed.

The aim of the thesis will be to estimate steam chamber volume and gas phase mobility by using pressure falloff tests of vertical well. Falloff tests are simulated by shutting-in the injector and recording the wellbore pressure with time. Injection rate, injection time and steam injection quality relation with swept volume and gas phase mobility are shown.

Definition of heavy oil, heavy oil reservoirs and their recovery and, detailed description of the SAGD (Steam Assisted Gravity Drainage) process, is included in literature review in Chapter 1. In Chapter 2, production techniques and recovery of oil sands are discussed in detail. In Chapter 3, thermal well test, pressure transient analysis, and falloff test are discussed. The simulation and application of case model, results and comprehensive discussion of the analyses and results is described in Chapter 4 and finally, conclusions are given in Chapter 5.

2. PRODUCTION TECHNIQUE AND RECOVERY OF OIL SANDS

2.1 Recovery of Oil Sands

In 1929, the Dominion of Canada issued a patent to Karl A. Clark (Url-6) for the hot-water extraction process for separating bitumen from oil sands. Butler (1982) introduced a method to develop oil sands recovery by using SAGD. Recovery of oil sands is done by open-pit mining and in-situ drilling methods as shown in Figure 2.1.

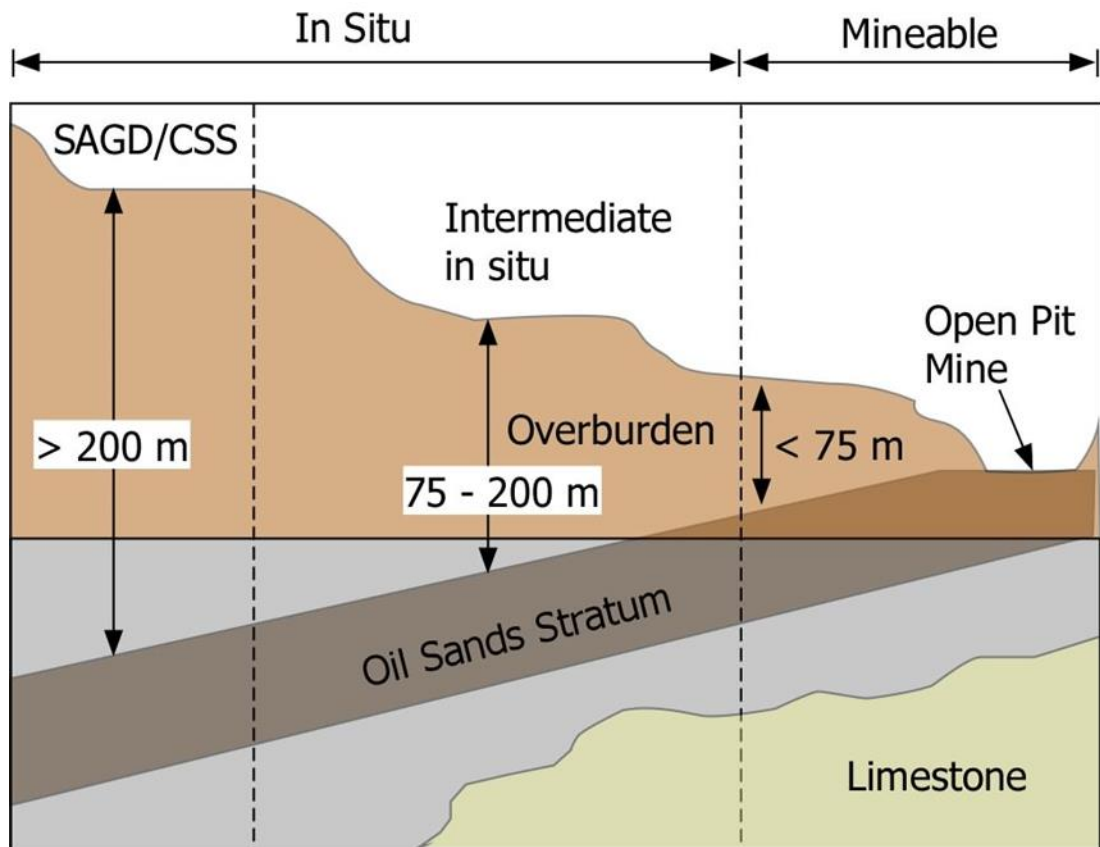


Figure 2.1 : The extraction techniques employed in oil sands recovery (Url-7).

Open-pit mining is similar to many coal-mining operations. Large shovels scoop the oil sands into trucks, which take it to crushers, where the large clumps of clay are broken down. The oil sands is then mixed with water and transported by pipeline to a plant, where the bitumen is separated from the other components. Tailings ponds are an operating facility common to all types of surface mining. In the oil sands, tailings consisting of water, sand, clay and residual oil are pumped to these basins or ponds; where settling occurs and water is recycled for reuse in the process. When the ponds are no longer required, the land will be reclaimed. In-situ drilling is 80% of oil sands

reserves that are too deep to be mined, so are recovered in place, or in-situ, by drilling wells (Banerjee, 2012).

Drilling (in-situ) methods create minimal land disturbance and do not require tailings ponds. There are two in-situ drilling methods:

(a). Cyclic steam stimulation (CSS) is Canada's largest in-situ bitumen recovery project used at Cold Lake. According to Figure 2.2 steam injected down the wellbore into the reservoir heats the bitumen, followed by a soak time, and then the same wellbore is used to pump up fluids. At Cold Lake, about 3200 wells are currently operating from multiple pads, with two above ground pipelines, one to deliver steam and the other to transport fluids back to the processing plant.

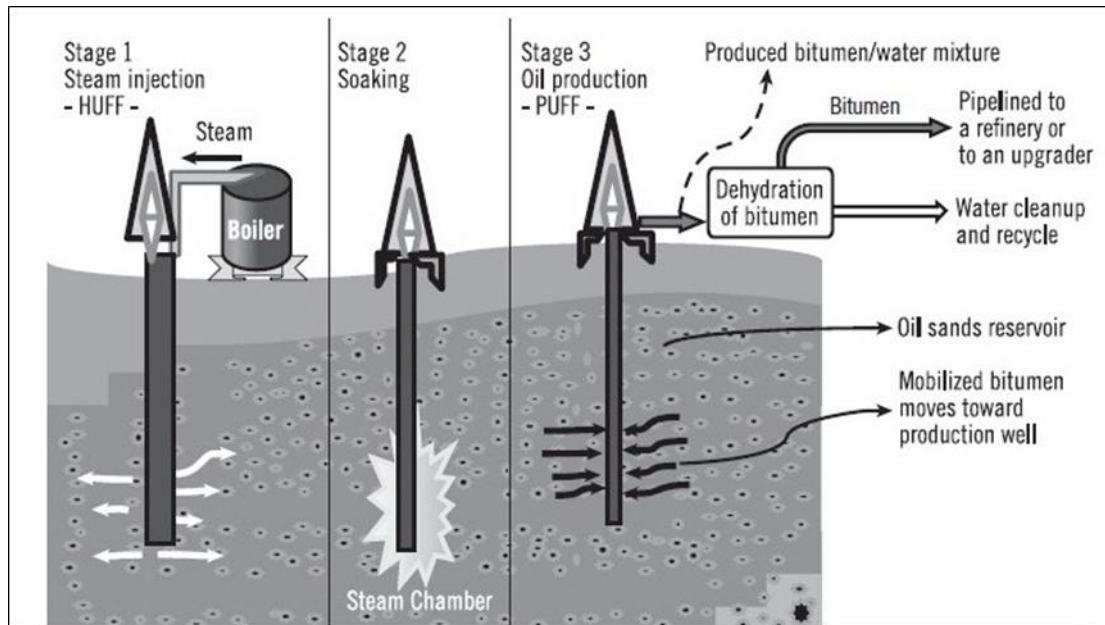


Figure 2.2 : Cross-sectional view of the CSS concept (Banerjee, 2012).

(b). Steam-assisted gravity drainage (SAGD) is originally conceived by Butler (1982). Horizontal well pairs (2300 ft long with 15-20 ft vertical separation) are drilled from surface pads to intersect bitumen pay as seen in Figure 2.3.

2.2 The Steam Assisted Gravity Drainage (SAGD) Process

Among different thermal recovery methods, steam injection is the most widely used method. The concept of SAGD was introduced originally by Butler (1982). Steam Assisted Gravity Drainage (SAGD) is one of the most important thermal recovery techniques applied in Alberta in the last three decades. SAGD is a thermal recovery

process for which two wells, one horizontal and one vertical, should be drilled. The injection well is 5 meters above of production well. Steam is injected from the upper well into the formation to reduce the viscosity of bitumen. In the SAGD process, by injection of steam in the reservoir, around and above the horizontal injection well, steam chamber is created. Usually, the injected steam contains about 80% steam and 20% water, and is injected through the injection well at a temperature above 390 °F and a saturation pressure above 435 psia to provide high quality steam to mobilize the bitumen. When steam is injected into the reservoir, heat is transferred to the oil-bearing formation, the reservoir fluids, and some of the neighbor cap rock. Due to this heat loss, some of the steam condenses to yield a mixture of steam and hot water.

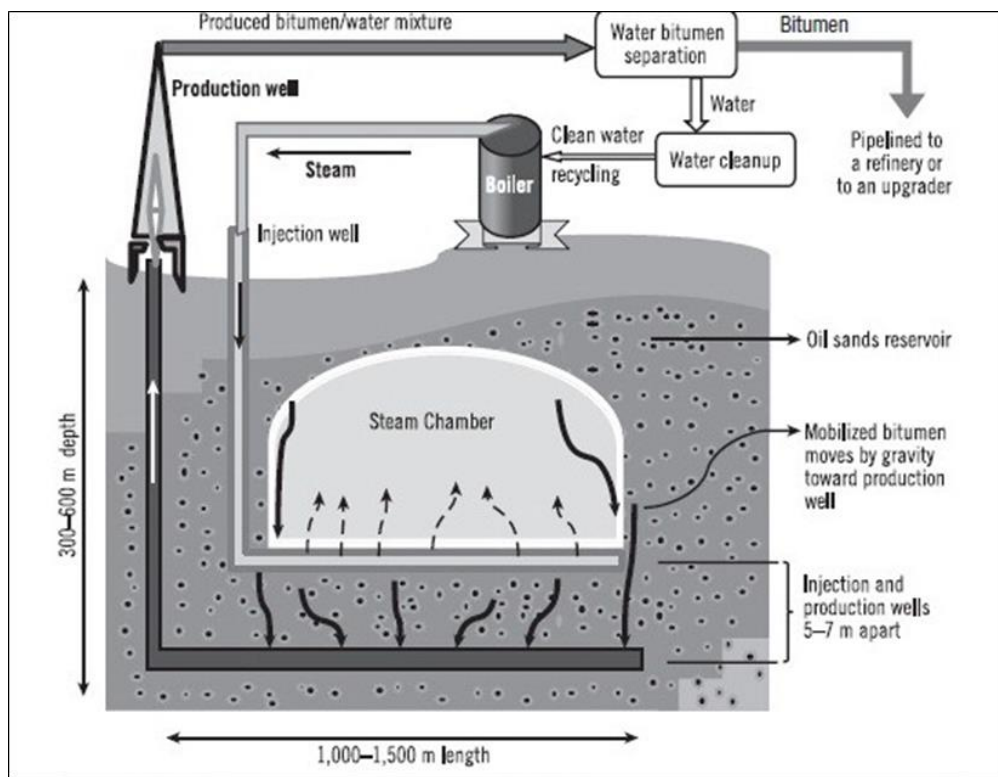


Figure 2.3 : Cross-sectional view of the SAGD concept (Banerjee, 2012).

As the steam chamber expands upward and laterally from the injection well, viscous hydrocarbons in the reservoir, are heated and mobilized especially at the margins of the steam chamber, where the steam condenses and heats a layer of viscous hydrocarbons by thermal conduction. The mobilized hydrocarbons and condensed water drain under the effects of gravity, moving toward the bottom of the steam chamber, where the production well is located. The mobilized hydrocarbons are collected from the production well. The rate of steam injection and the rate of hydrocarbon production may be controlled with the growth of the steam chamber. It

is necessary to ensure that the production well remains located at the bottom of the steam chamber in an appropriate position to collect mobilized hydrocarbons, if possible far from the water in a clean part of the reservoir.

Start-up is a process to bring the SAGD well pair in fluid communication with each other and to initiate a steam chamber. It is aimed at achieving uniform and active drainage along the full length of the well pair through the start-up process. Typically, the start-up phase takes three months or more, until communication is established between the two horizontal wells. Importantly, for efficient production in the SAGD process, conditions in the injection and production wells need to be maintained, so that steam does not simply circulate between the injection and production wells, short circuiting intended SAGD process. This may be achieved by controlling steam injection so that the bottom hole temperature at the production well is below the steam temperature.

Sahuquet et al. (1990) simulated a horizontal injector and vertical producer process because several tests showed that steam injection through a vertical well was not efficient due to the low permeability. According to Sedaei and Rashidi (2006) literature review, there are just a few studies applying SAGD in fractured reservoirs and they simulated SAGD in an Iranian carbonate fractured.

A considerable part of the SAGD process is the initiation of a steam chamber in the reservoir. The typical approach to initiating the SAGD process is to operate the injection and production wells simultaneously with high-pressure steam. However, steam is independently circulated in each of the wells during this start-up phase, heating the hydrocarbon formation around each well by thermal conduction. Independent circulation of the wells is continued until efficient fluid communication between the wells is established. Once the fluid communication is established between the wells, the injection well is dedicated to steam injection while the production well is dedicated to oil production only. Steam is always injected below the fracture pressure of the rock mass. Also, the production well is often stopped to maintain the temperature of the bitumen production stream just below saturated steam conditions to prevent steam vapor from entering the wellbore and diluting oil production ; this is known as the SAGD “steam trap” (Banerjee, 2012).

The SAGD process is able to recover 55% of the original bitumen-in-place. Depending on the characteristics of the reservoir, sufficient pressure must be maintained to lift the produced fluid to the surface. For example, a minimum pressure difference of 200 psi is required in order to lift the fluid (bitumen/water mixture) more than 1000 ft to the surface. The volume of water handled in the SAGD operation represented by the steam-oil ratio (SOR), which is about 3.0; it means it takes three barrels of water equivalents of steam to recover one barrel of bitumen. At the start-up phase, the SOR is much higher than 3.0; finally, it goes down, to about 3.0 at optimum conditions. However, producers are trying to decrease the SOR to decrease their operating costs.

2.2.1 SAGD mechanism

An analytical equation is used to predict the rate of oil drainage of the steam chamber expressed by Butler's gravity-drainage theory, with some assumptions that only steam flows in the steam chamber, oil saturation is residual, oil drains along the vertical steam chamber, and heat transfer ahead of the steam chamber to cold oil is only by steady-state conduction (Butler (1994) and Akin (2005)).

$$q = 2L \sqrt{\frac{1.3\phi\Delta S_o k g \alpha h}{m\nu_s}} \quad (2.1)$$

where L is the length of the horizontal well, ϕ is the porosity of the formation, ΔS_o is the difference between initial oil saturation and residual oil (mobile oil saturation) and k is the effective (vertical) permeability for the flow of oil. g is the acceleration due to gravity, α is the thermal diffusivity, h is the thickness of the reservoir or bitumen column, m is the Butler parameter and ν_s is the bitumen kinematic viscosity at steam temperature. The mechanism of SAGD is illustrated schematically in Figure 2.4. During the rise of the steam chamber (countercurrent flow period), the oil production rate increases steadily until the steam chamber reaches the top of the reservoir. At later stages of the process, when the chamber reaches the top of the reservoir, the production rate of oil is controlled by the lateral expansion of the steam chamber (co-current flow period). During this phase of the process, production rate declines and steam oil ratio (SOR) eventually increases because of heat loss to the overburden (Sedaei and Rashidi, 2006).

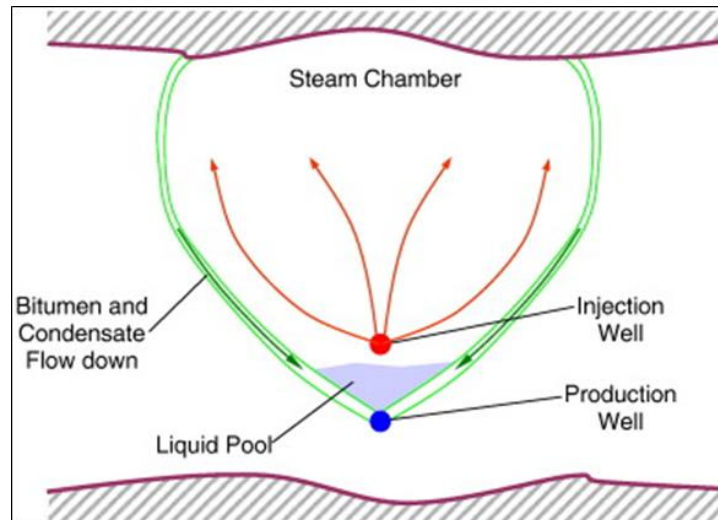


Figure 2.4 : Basic description of SAGD process (Gates and Leskiw, 2008).

2.2.2 SAGD design issues

Farouq Ali (1997) and Singhal et al. (1998) mentioned some limitations of SAGD as follows: (1) The theory depends on the single phase fluid flow, (2) Only steam flows in the steam chamber and oil saturation being residual, (3) The heat transfer ahead of the steam chamber to cold oil is conduction only, (4) Sand control may be necessary, (5) There is a hot effluent water cut production, (6) Frequent changes in operating regimes and high operating costs occurs, and (7) Decline of production at late stages in SAGD, greatly improves reservoir contact and well productivity. To achieve a reasonable oil production rate, one would choose a pair of horizontal well 1500-3500 ft long. The horizontal producer placed close to the base of reservoir pay, to maximize the reservoir drainage volume, and the injector drilled above and parallel to the producer. The vertical separation of the wellbores is 13-20 ft for Alberta oil-sands formation. The oil production rate for Alberta oil sands reservoir is in the range of 0.5-2 bbl/day per feet of wellbore. As in all thermal recovery processes, the SAGD process is also energy intensive. The energy balance analysis shows that in general the energy injected the steam can be roughly, divided into three equal streams: one-third retained in the steam chamber, one-third dissipated to formation rock outside the steam chamber, and one-third produced to surface (Yee and Stroich, 2004). For the process to be economical, the energy efficiency measured in terms of cumulative steam to oil ratio (CSOR) is generally in the range of 2-4 barrels of steam per barrels

of oil. SAGD for heavy oil recovery can achieve a recovery factor of 60% in general, or even as high as 70-80 % in some favorable reservoirs (Wong et al., 1999).

If we determine the swept volume in a thermal oil recovery process, we can solve the primary concern. For an accurate early stage economic evaluation of the field operation, we need to estimate the swept volume at intermediate stages of the operation either in-situ combustion or steam injection. The volume occupied by steam is a measure of the heat loss from the hot injection zone, if the cumulative steam injected is known (Satman et al., 1980). As SAGD process uses horizontal wells; permeability anisotropy will play a strong role in recovery (Peaceman, 1983).

2.2.2.1 Well spacing

More work has been done on the spacing between wells. Previous experiences and simulations have shown that well placement affects the recovery factor and breakthrough time. Some reservoir and operating parameters of three major oil sand projects in Alberta, Canada were studied (Shin and Polikar, 2005) numerically, one of which was the injector to producer spacing. The results showed that an increase in the injector to producer spacing leads to an increment in the recovery factor, however, it prolongs the breakthrough time. For example, in 5 meter well spacing, the recovery factor was 42 % and increased to 49 % for 15 meter well spacing. Sawhney et al. (1995) carried out an extensive experimental, theoretical and scale up study of vertical injection SAGD. They concluded that horizontal injection SAGD is more efficient than vertical injection SAGD in the case of Cold Lake reservoir. The effect of vertical spacing has also been studied. This was examined by Edmunds and Gittins (1993) and is shown in Figure 2.5. With larger vertical spacing, more time is required to initiate communication between the injector and the producer. Ultimately, this is an issue of timing and changes in rates.

2.2.2.2 Implications of thief zone

For a SAGD design, the thief zone represents a serious technical problem. The steam chamber must be run at lower temperatures and pressures to prevent the loss of steam. Steam loss can not be prevented completely. This can represent a real loss in the potential economics of the project.

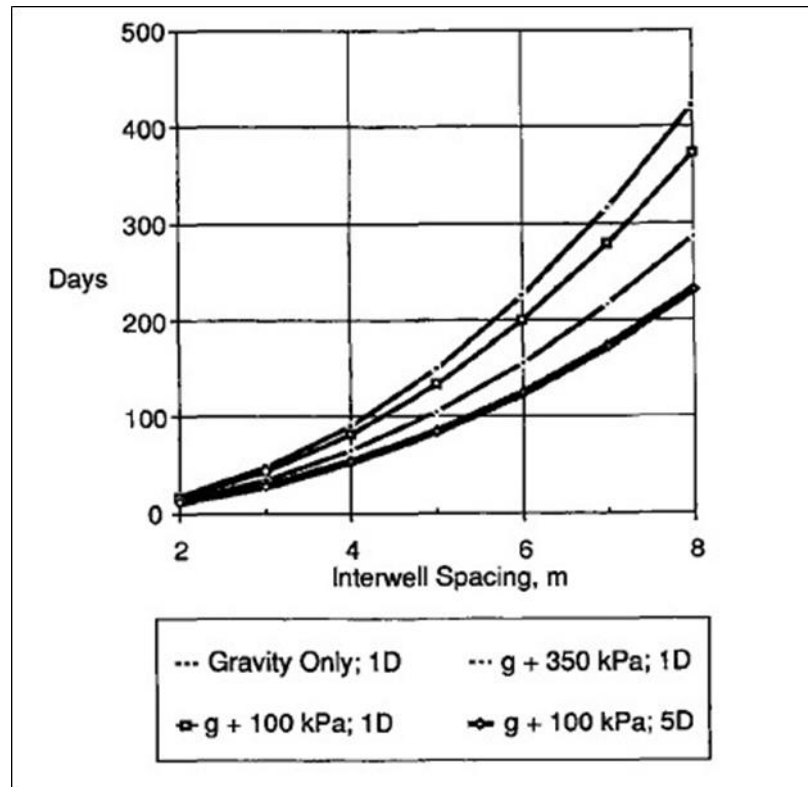


Figure 2.5 : SAGD start-up time versus spacing and potential difference and permeability (Edmunds and Gittins, 1993).

2.2.3 Criteria for evaluating performance

The main criteria for evaluating SAGD are discussed below.

Breakthrough Time: The time that it takes for communication to occur between the horizontal injection and production wells. It is a function of the distance between the injector and producer and input heat.

Production Rates: Higher rates have relationship with revenue, this alters economics directly, the maximum rate, usually indicates the overall level for the production forecast.

Recovery Factor: This indicates the total expected amount of resource to be recovered. Actually, high recovery factor does not necessarily translate into high economical efficiency.

Steam-Oil Ratio (SOR): This is an indicator of efficiency of bitumen's recovery but usually the Cumulative Steam-Oil Ratio (CSOR) is used. It inversely describes the

overall efficiency (i.e., the lower SOR implies higher efficiency of SAGD process). Generally, at the beginning of the steam injection process, the SOR is rather high. However, towards the end of the injection process, the amount of SOR dictates the point in which the operation should be finished, to remain economically viable.

Rise Rate: Rise rate can show the SAGD chamber performance. This is normally expressed in cm/day or in/day. It is not necessary for the chamber shapes to be the classic discontinuities, the upside-down triangular, or of significant dimensions. It can affect the rise rate without really reflecting whether the SAGD process is working. However, in case of sufficiently homogeneous reservoir, this can be a useful indicator.

2.3 Horizontal Well

In the 1970s or earlier, almost all producers and injectors were drilled as vertical or deviated wells in oil and gas reservoirs. Since 1990s, the industry try to design and develop the operation of horizontal well technology. In recent times, an increasing number of horizontal wells have been drilled to achieve better reservoir performance. In the last few years, many horizontal wells have been drilled around the world. These wells contact thousands of feet of net pay in the horizontal direction, and contribute substantially to well productivity. As an injection well, a long horizontal well provides a large contact area, and therefore enhances well productivity. The major disadvantage is that only one pay zone can be drained per horizontal well. The other disadvantage of horizontal wells is their cost. Typically, it costs about 1.4 to 3 times more than a vertical well, depending upon drilling method and the completion technique employed. An additional factor in cost determination is drilling experience in the given area; the first horizontal well costs much more than the second well. As more and more wells are drilled in the given area, an incremental drilling cost over a vertical well is reduced.

Performance of conventional SAGD horizontal well completions can have a significant impact on formations with low vertical permeability and mudstone layers hindering vertical drainage. Also, the timely growth of the vertical chambers can be affected by the shallow depth, cap rock integrity, and/or thief zone issues, the lower

operating steam pressure for SAGD completions. There is a direct correlation between the length of horizontal wellbore and well productivity enhancements, validated in numerous field studies. A study on the data from 1306 horizontal wells in 230 fields, indicated the highest productivity enhancements is achieved in fractured reservoirs, in which up to a 12-fold increase in rate was observed (Levitan, 2001).

The recovery process utilizes horizontal producers to respond to steam injected from vertical wells which were located above the producers in the pay to drain oil between and beneath wells. Jahanbani et al. (2011) also after analyzing the application of thermal well testing method for vertical and horizontal steam injection wells for Athabasca oil sample, concluded horizontal wells are suitable choice for efficient oil recovery, especially from thin reservoirs.

Pressure drop along the horizontal wells and between the injector and producer may have a major impact on SAGD process performance. When the pressure drop between the injector and producer exists, the downhole producer vapor production rate will increase noticeably. Oil production rate is lower and SOR is higher, without adequate vapor production. Additionally, increase in vapor production rate can affect pad facility design, and can result in an increase of cost as more vapor handling capacity. Moreover, pressure drop inside the injector well may alter the steam distribution requiring more steam injection into the heel section. The impact on oil production is limited as steam can move relatively easily inside the steam chamber. Due to gravity, anisotropy and heterogeneities, the steam chamber for a horizontal well may not be symmetric around the wellbore. The resulting asymmetry can mask parts of pseudo steady state flow regime, and lead in unreliable calculations.

2.3.1 Horizontal injection wells

Figure 2.6 shows the initial stage of SAGD. The steam chamber grows upward and sideways from a horizontal injector above a horizontal producer in a bitumen reservoir. During the initial phase of operation, the steam chamber grows upwards and then spreads down the overburden. The broken line in the right hand diagram in the figure shows the steam chamber profile during an initial stage. If the viscosity of the

in-situ oil is a few thousand cp, it is possible to place the injection and production wells wide apart.

2.3.2 Vertical injection wells

In bitumen reservoirs, one or more vertical injectors can be implemented, as shown in Figure 2.7. Imperial Oil has demonstrated this concept at Cold Lake. An advantage of such arrangement is the decrease in costs, as a vertical injector is cheaper than a horizontal one. In addition, it may be practical to utilize existing vertical wells, instead of drilling new ones. Once the steam chamber is established, the height of steam injector can be changed; this is an advantage of vertical injectors. In a vertical injector configuration, the required pressure gradient to move the steam to the interface, usually elevate the oil drainage. The important disadvantage of vertical injection wells is that the steam chamber has to grow along the direction of the axis of the horizontal well as well as transversely. Therefore, the effective length of the production well, particularly in the early stages, may be less than its physical length.

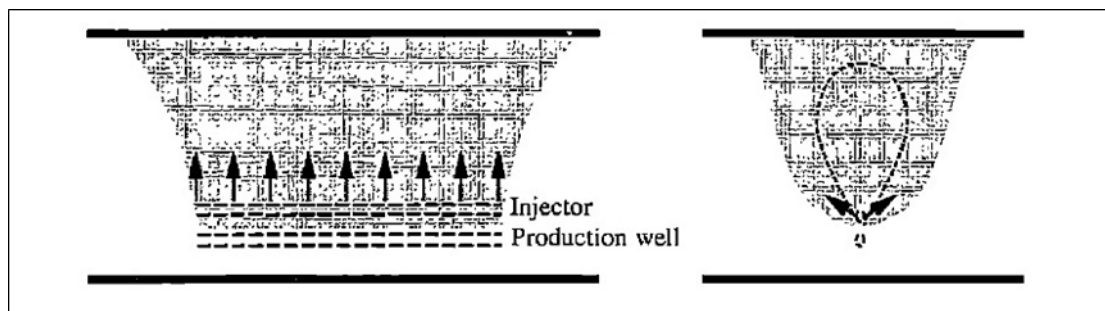


Figure 2.6 : Growth of steam chamber with horizontal producer and injector (Sawhney et al., 1995).

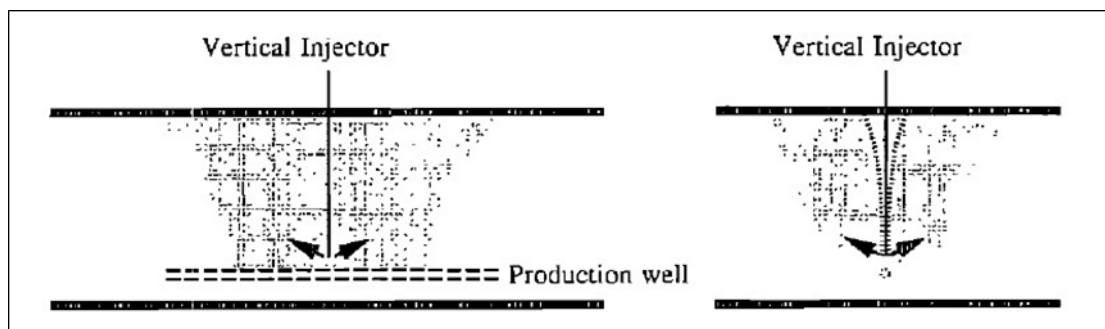


Figure 2.7 : Growth of steam chamber with horizontal producer and vertical injector (Sawhney et al., 1995).

3. THERMAL WELL TESTING

In this section, the results of viscosity and density measurement of (Jahanbani et al., 2012b) and (Mehrotra and Svrcek, 1986) are presented. The bitumen samples are obtained from an oil sand in Athabasca region. The decrease in viscosity of oil, causes its mobility to increase. The oil mobility is the ratio of the effective permeability to the oil flow to its viscosity. This is given by equation (3.1):

$$\lambda_o = \frac{k_o}{\mu_o} \quad (3.1)$$

where λ_o is the oil mobility in md/cp, k_o is the oil effective permeability in md and μ_o is the oil viscosity in cp.

3.1 Viscosity and Temperature

By decreasing the viscosity of oil, the displacement of oil by another fluid is much easier. Actually, the oil may even drain to the bottom layers by gravity, if the viscosity reaches small values. Khan et al. (1984) proposed the empirical correlation between the effect of temperature and the viscosity of gas free Athabasca bitumen. One of their correlations is equation (3.2), is plotted on Figure 3.1:

$$\ln[\ln(\mu)] = c_1 \ln T + c_2 \quad (3.2)$$

μ is dynamic viscosity of heavy oil sample in cp at atmospheric pressure and temperature $T(^{\circ}K)$. The constant c_1 and c_2 are empirical and can be found by the least square parameter estimation technique, they are respectively -3.5912 and 22.976.

Heat transfer by convection is much faster than heating by conduction. Heating by convection occurs when steam flows in the fractures within the reservoir. Then, it is transmitted by movements of particles within the steam and heats the occupied

volumes. Since pumps inject the steam to the subsurface, the process is named forced convective heating. The heat transfer by convection is expressed by equation (3.3):

$$u_T = u\rho c(T - T_r) \quad (3.3)$$

Here u_T is the convective heat flux in BTU/ft²d, u is the volumetric flux in ft/d, ρ is the steam density in lb/ft³, c is isobaric specific heat in BTU/lb°F, T is steam temperature in °F and T_r is the reservoir temperature in °F.

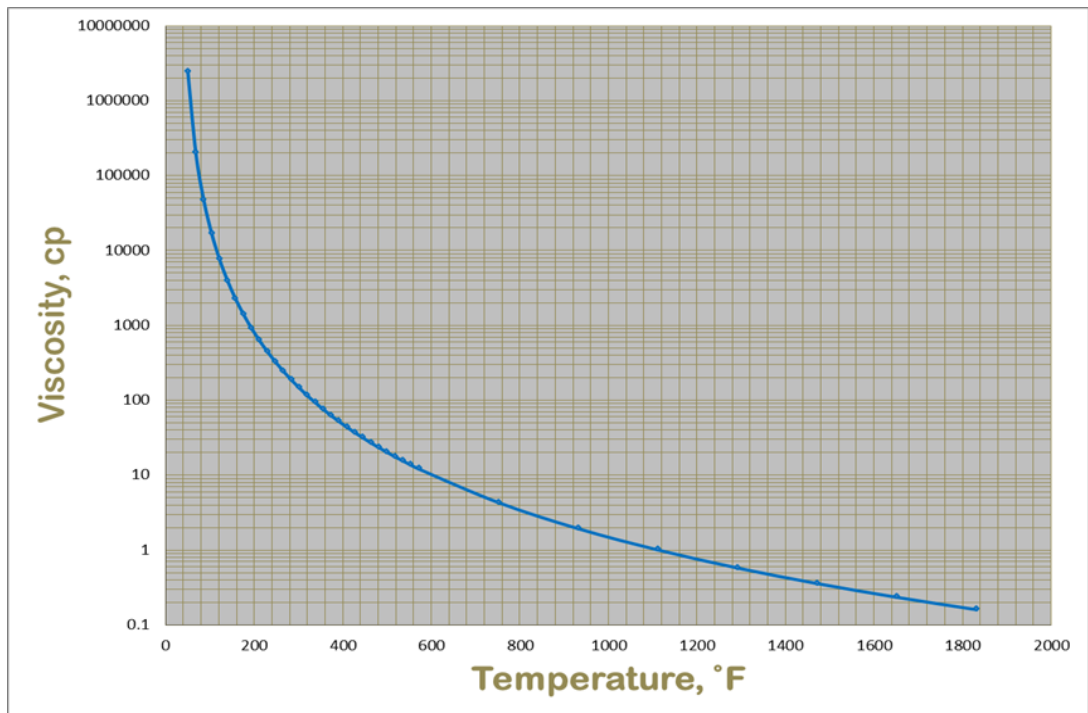


Figure 3.1 : Viscosity of Athabasca bitumen versus temperature (Jahanbani, 2012b).

Producing steam is the majority of the cost in SAGD. The material balance can be used directly in the calculation of efficiency. Not all produced heat can be recovered, however, improved efficiency in recovering heat will significantly reduce steam generating costs. To illustrate the heat balance equation clearly, the total heat injected, Q_i , mass injected, steam quality, latent heat of vaporization and temperatures of steam and reservoir need to be introduced, according to equation (3.4). Steam quality determines the capacity of heat stored in the water vapor phase. Latent heat of vaporization is how much extra heat steam can hold compared to water at the same temperature.

$$\int_0^t Q_i (\text{Heat Injection}) dt = \int_0^t Q_D (\text{Heat Delivered}) dt + \int_0^t Q_L (\text{Heat Lost}) dt \quad (3.4)$$

The combination of conductive and convective heat transfer coefficients is the heat transfer coefficient that is the reciprocal of the overall specific thermal resistances of system. The higher the heat transfer coefficient, i.e. the more heat is transferred, the less the thermal resistance is. Usually in practice, the resistance of one component dominates the total thermal resistances of the system. If the dominant resistance is determined, then, the calculations can be simplified greatly by cancelling out the other terms that have negligible effects. For most cases, the rate of heat loss is considered steady-state per unit length of pipe and is directly proportional to the difference in temperature between steam and the surrounding medium but inversely to the overall specific thermal resistance of the system. Therefore, for a given reservoir, it is possible to calculate the amount of heat injected followed by heat loss analysis to determine how much heat is lost, and thus, know how much heat is in the reservoir. These calculations clarify important numbers such as how much steam to inject, at what rates, for how long and at what quality. The calculations also clarify important numbers in heat loss analysis such as rate of heat lost to the formation whether by convective or conduction mechanisms, diffusion or conductivity, and how fast the loss is.

The temperature profile in the reservoir, gradual distribution of steam temperature in the productive zone, the overburden and the underburden are shown in Figure 3.2. At day 1, the temperature around the injector is at steam temperature and it starts to decrease as it moves away from the well in both directions until it reaches the original reservoir temperature. After 10 days, more areas are heated and this can be observed by the increase of the temperatures near the injector. After 100 days, the temperature profile looks uniform, and if the injection lasts for another 100 days, the profile will become more constant. Temperature behavior around injector in left hand side of Figure 3.2 is similar to reservoir temperature profile with that in different distance temperature changes become constant.

3.2 Steamflood Front Mechanism

Extensive work on these issues has been done with respect to both water and steam

flooding, with good matches obtained between analytical and laboratory experiments. An example of this is shown in Figure 3.3.

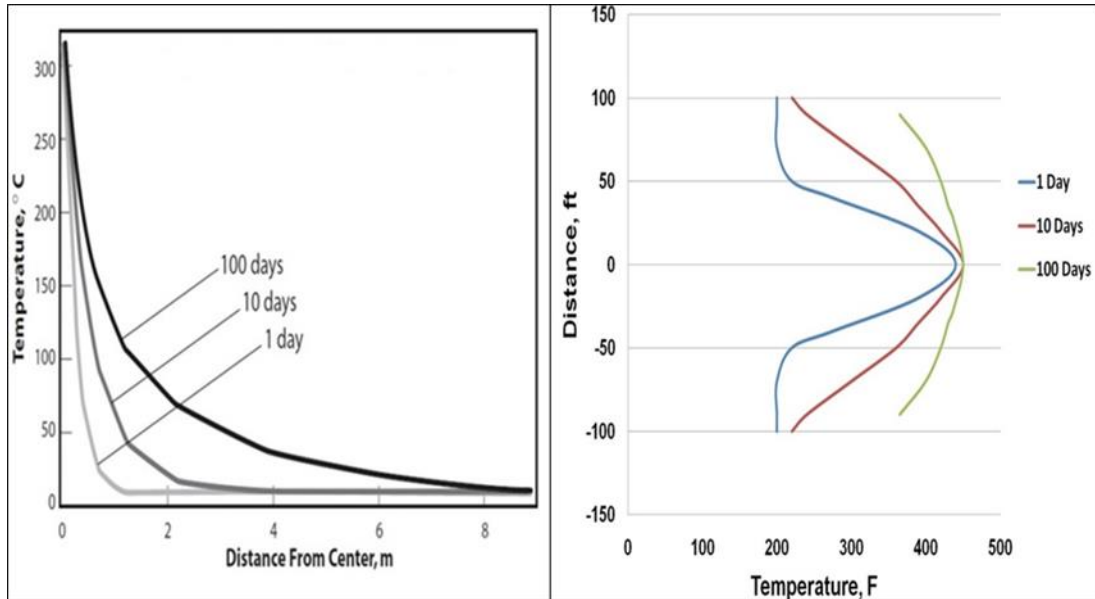


Figure 3.2 : Temperature profile in the reservoirs and around the injector (Url-8).

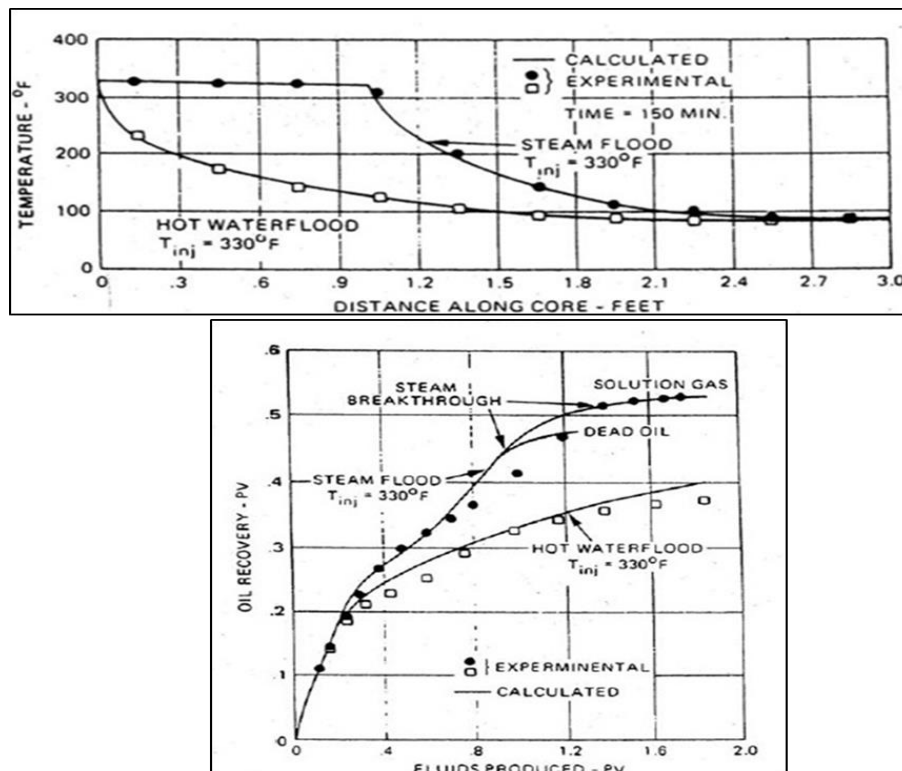


Figure 3.3 : Steamflooding advance (Satter et al., 2008).

Historically, steamflood work has concentrated on the interface between the oil and the bitumen. It is based on the assumption that the steam will condense at the cold bitumen front. This process would be dominated by water-oil relative permeability

curves. Behind this region is saturated steam, and this process will be affected by gas-bitumen relative permeability. It is likely that the process in a SAGD chamber involves recovery both at the interface and in the steam chamber during a period. Oil viscosity can be measured at the heated zone temperature by either empirical formula or in the lab, using rock properties from rock samples extracted from the same zone. The oil flow rate is then, estimated based on the Darcy law by equation (3.5):

$$Q = - \frac{1.127 \times 10^{-3} k A \Delta P}{\mu L} \quad (3.5)$$

where Q is the oil flow rate in bbl/day, k is the effective permeability of oil in md, A is the cross-sectional area to flow in ft², ΔP is the pressure differential between two points in psia, μ is the oil viscosity in cp and L is the length in ft which pressure drop is occurring in. Then, for given time of steam injection, the engineer can predict the amount of oil recovered.

Thermal well testing methods for determination of swept volume, has not been the focus of studies on horizontal wells, and, except in Issaka and Ambastha (1992) and Shamila et al. (2005), studies were focusing on vertical test. Satman et al. (1980) and Eggenschwiler et al. (1980) gave an estimate of the steam zone properties and swept volume using falloff test, assuming two regions of highly contrasting fluid mobility and an impermeable boundary interface in a composite reservoir. Consequently, for a short duration, the swept zone acts as a closed reservoir, during which the pressure response takes the form of a pseudo steady state behavior. Jahanbani et al. (2011) investigated the feasibility of thermal well test analysis and effects of different parameters and simulated pressure falloff testing by using a numerical thermal simulator. Jahanbani et al. (2011) generated pressure falloff test data, and then analyzed it to calculate swept volume and reservoir parameters. Different gridblock models are designed and results of this study show that the swept volume, swept zone permeability and skin factor can be reasonably estimated from pressure falloff tests. Viscosity of Athabasca heavy crude sample was measured in the lab using a rotational viscometer up to 570 °F. Bitumen sample molar mass was measured by cryoscopy. Density at standard conditions was measured by a density-measuring cell. The applicability of thermal well testing method to horizontal wells with application to SAGD process for a typical Athabasca heavy oil reservoir was investigated and

effect of several SAGD operating parameters on well test results, were studied by (Jahanbani et al., 2012). Utilizing thermal well testing method, one can inexpensively determine flow capacity and swept volume in thermal recovery process. The thermal well testing method in steam flooding projects is pressure falloff testing based on (Satman et al. 1980). In field operations, the swept volume has been determined by coring and/or temperature observations made at wells during passage of the displacement front. These methods are, however, expensive and time consuming (Akhondzadeh and Fattahi, 2014). Different methods for estimation of swept volume from pressure falloff test include the deviation time, intersection time, type curve matching, and pseudosteady state methods. Kazemi (1966) solved pressure falloff-test model numerically, to calculate the distance to the burning front. However, horizontal well testing is more complex than vertical well testing, but the employment of horizontal wells instead of vertical wells helps to increase the oil production, because provides large contact area for the reservoir and also reduces gas and water coning problems, and also the drilling technology of horizontal wells is economical.

3.3 Relative Permeability

One of the most important input variables for numerical reservoir simulation is the relative permeability. The relative permeability curves and residual fluid saturations are required in order to estimate the oil production rate and ultimate recovery (Polikar et al., 1990). In the simulation study considered in this thesis, the water/oil and gas/oil relative permeability curves used (Coats et al., 1974) are shown in Figures 3.4 and 3.5, respectively. The relative permeability characteristics of the oil, gas, and water phases present in the reservoir may have a pronounced effect on reservoir performance during enhanced recovery operations. Certain relative permeability curves may exhibit high residual oil saturation or an abrupt increase in the relative permeability of the water phase when the latter becomes mobile. These reservoirs may not prove to be good candidates for enhanced recovery. Ultimate recovery from reservoirs with unfavorable relative permeability trends could be comparatively less. Results obtained from reservoir simulation studies depend heavily on the phase relative permeability data used.

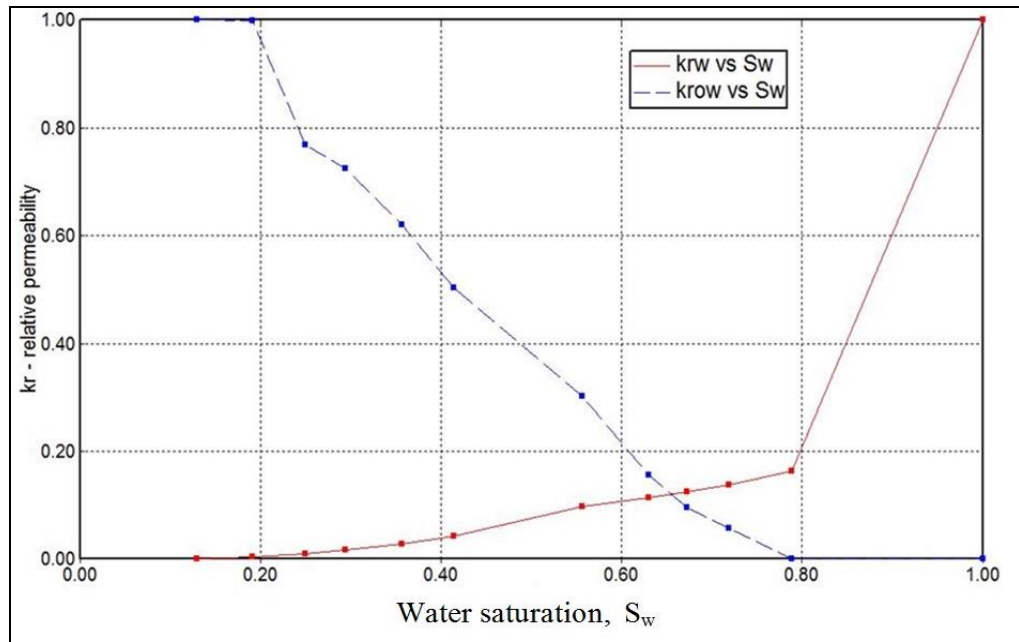


Figure 3.4 : Water/oil relative permeability curve (Coats et al., 1974).

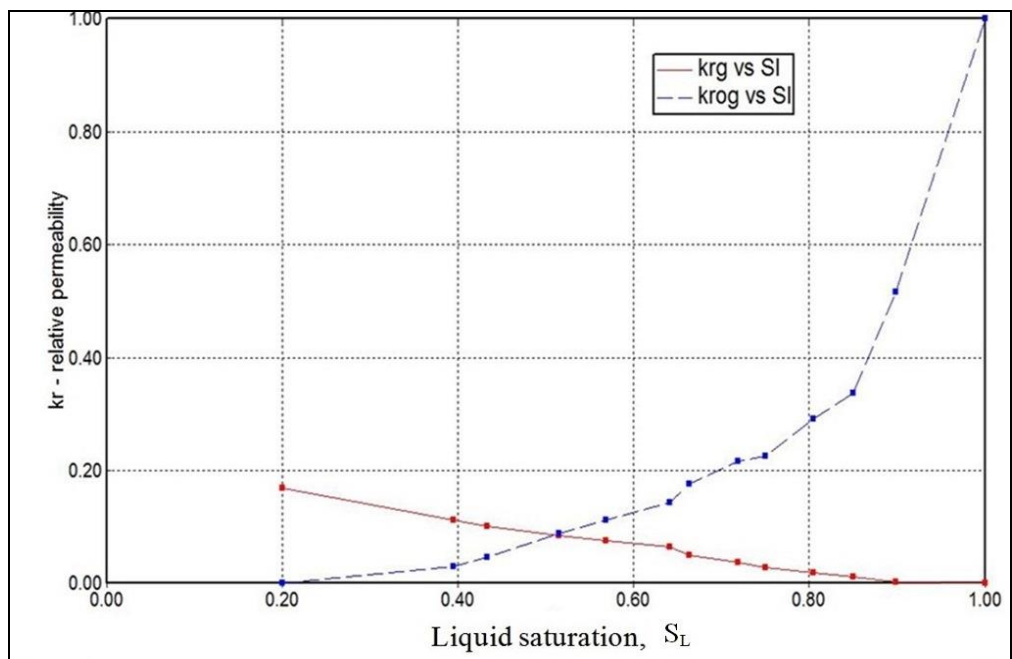


Figure 3.5 : Gas/oil relative permeability curve (Coats et al., 1974).

3.4 Transient Well Test

By using the transient well test, evaluating and enhancing well performance become easier because it helps characterizing a reservoir to identify faults, fractures, reservoir boundaries, fluid communication between layers, and tracking of fluid fronts, to name a few applications. Commonly referred to well testing, virtually all wells undergo some kind of pressure transient testing during various stages of their

productive lives. Any well that is drilled newly, is tested for assessing the future potential of the well. In some fields, reservoir performance is intensively monitored due to the existence of complex geology, an ongoing enhanced recovery operation, or monitoring of specific production issues. We create a change in the well rate and analyze the response of the transient pressure, by carefully monitoring using electronic recording devices, followed by detailed computer analysis. There is two ways to accomplish this; either by the shut-in of an active well, or flow at predetermined rate from a well that was inactive prior to drawdown.

There are many types of pressure tests, but not limited to, the following: pressure buildup (PBU) test, pressure falloff (PFO) test, step rate test, pulse and interference test, dynamic formation testing. Depending on the reservoir properties and the dimensions, up to four different transient flow regimes may occur for a horizontal well employed in thermal flooding operation: (1) Early Radial Flow Regime: occurs immediately after the well starts to flow (no wellbore storage effects). (2) Early Linear Flow Regime: occurs after the early radial flow if the well is significantly longer than the reservoir thickness. (3) Late Pseudoradial Flow Regime: This is the flow regime period we are interested in order to determine the swept volume. (4) Late Linear Flow Regime: This period may follow the pseudoradial period provided the reservoir length is significantly larger than its width. For a vertical well in an infinite radial reservoir, Early Linear Flow Regime does not occur and a Late Radial Flow Regime instead of Late Linear Flow Regime is observed.

Falloff tests are conducted in fluid injection wells, and are usually part of a pressure maintenance or enhanced recovery program in a petroleum reservoir. The well is first injected at a constant rate for a sufficient period to achieve stabilization in injection pressure, followed by shutting in of the injector. As a result, the bottom hole pressure at the well begins to decline (falloff), which is recorded and analyzed. Conceptually, it is a mirror image of a buildup test, as depicted in Figure 3.6. Pressure fall off test is used to determine the pseudo-steady state flow.

3.5 Method of Analysis

The application of thermal well-test analysis methods for the estimation of permeability and swept volume, for vertical well under steam injection process, is

implemented in this work. This test will be used to estimate the volume swept (V_s) by steam injection from a single injector well into the formation. It is determined by plotting the falloff test bottom hole pressure (p_{ws}) versus shut-in time on a Cartesian plot, where the Pseudo Steady State (PSS) flow occurs in the latter portion of the that time. If the reservoir has a constant pressure outer boundary the Steady State (SS) flow rather than PSS occurs in the latter portion. It is performed under constant pressure in the reservoir, constant injection flow rate, after which the well is shut in to allow pressure build up to decline.

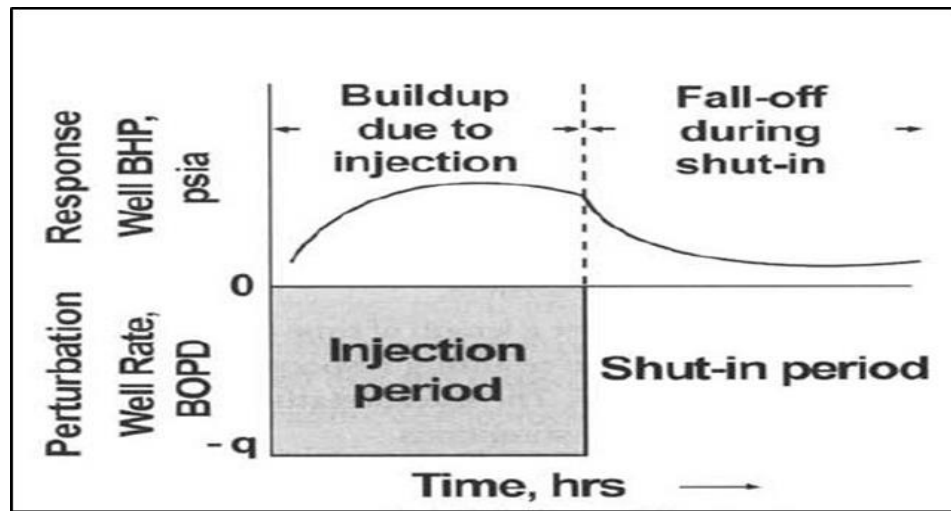


Figure 3.6 : Falloff test (Satter et al., 2008).

The MDH (Miller-Dyes-Hutchinson) method for the analysis of falloff data is used because the shut-in time is much less than the injection time in practical steam injection falloff tests. Pressure is plotted versus the logarithm of flowing time. For average steam properties evaluation, we applied liquid well testing analysis on steam fall off testing. Liquid well testing analysis is the popular thermal well testing method applied in practice. Jahanabani et al. (2012) indicated that real gas analysis, in fact is unnecessary because of the relatively small pressure changes common for steam pressure falloff testing.

Several transient flow regimes may be observed in falloff test. The possible flow regimes are: the early time region (ETR) of altered permeability caused by the wellbore storage effect, the middle time region (MTR) represents radial flow where formation permeability can be determined from the slope of a straight line and the late time region (LTR) reflects the effect of reservoir boundaries and heterogeneities as shown in Figure 3.7, (Lee, 1982).

3.6 Reservoir Simulation Model

The reservoir model considered in our study consists of a formation area of 160000 ft² and thickness of 175 ft. Reservoir is modeled as having five equal thickness layers and the injection well is supposed to be completed with partial completion in each layer as shown in Figures 3.8 and 3.9. The reservoir model is homogenous with single porosity equal to 35% and 63.23 lb/ft³ dead oil and 2400 cp viscosity.

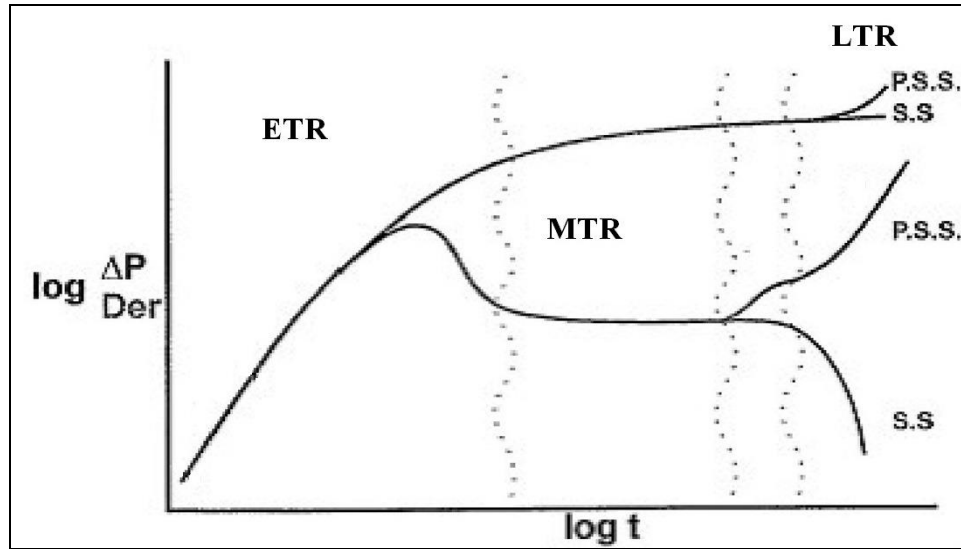


Figure 3.7 : Specific flow regimes within all categories in fall-off test (Lee, 1982).

Horizontal absolute permeability (k_i) is 700 md, vertical absolute permeability (k_k) is 70 md and absolute permeability in J direction (k_j) is 700 md. Steam is injected at a rate of 500 STB/day for 30 days into the reservoir until appreciable rock volumes are swept, then pressure falloff tests are simulated by shutting-in injection well (for one day) and reading the bottom hole pressures as a function of time. The injection flow rate is held constant. Heat loss is allowed from the formation to the upper and lower layers surrounding the reservoir. Irreducible water saturation is 20%, and initial oil saturation is 80%. Initial reservoir pressure is 700 psia, and temperature is 93° F. Simulation begins on 2014-08-21 and finishes on 2014-9-11 for an injection period of 30 days. The reservoir and fluid properties used in simulation studies are presented in Table 3.1. The thermal simulator, STARS (CMG 2012), is used to simulate falloff tests in this study. The grid cells in the directions of length, width and height are denoted by the letters i, j and k, respectively. The injection well is located in the center of the reservoir and displaying open intervals of the injection well as shown in 3D view of reservoir in Figure 3.9.

In this study, the gridblock sizes used are shown in Table 3.2. The 3D model is Cartesian system having $23 \times 23 \times 5$ gridblocks and the size of reservoir model is $400 \times 400 \times 175$ in width, length and height, respectively.

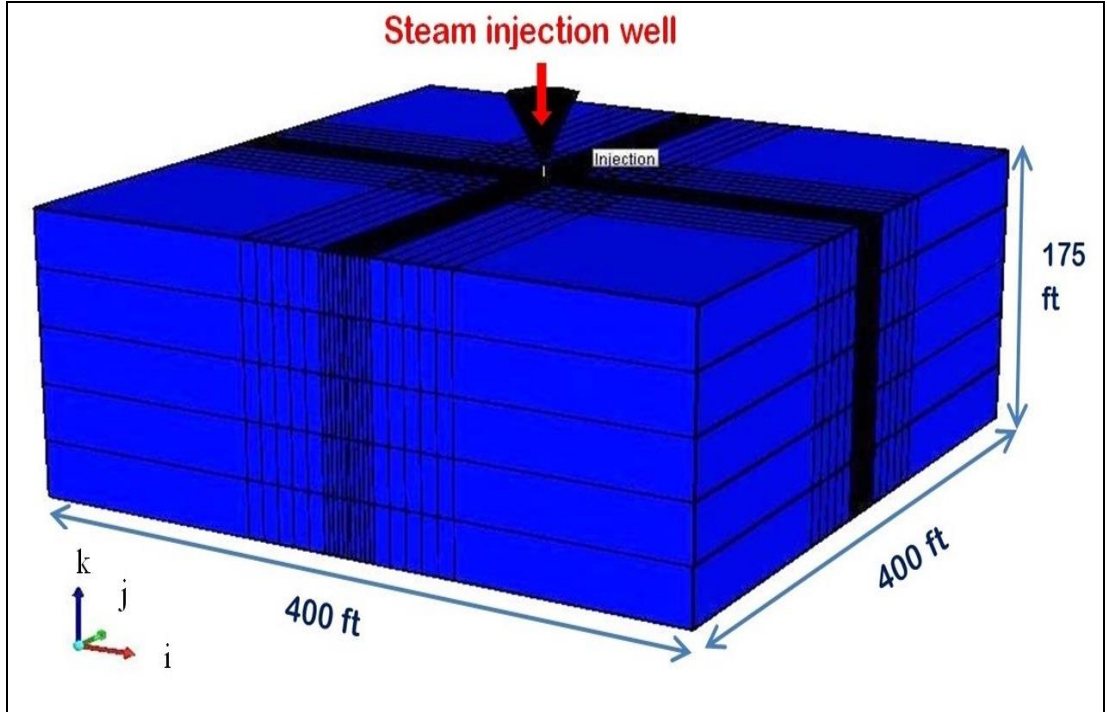


Figure 3.8 : 3D view of well configuration in the numerical simulation model.

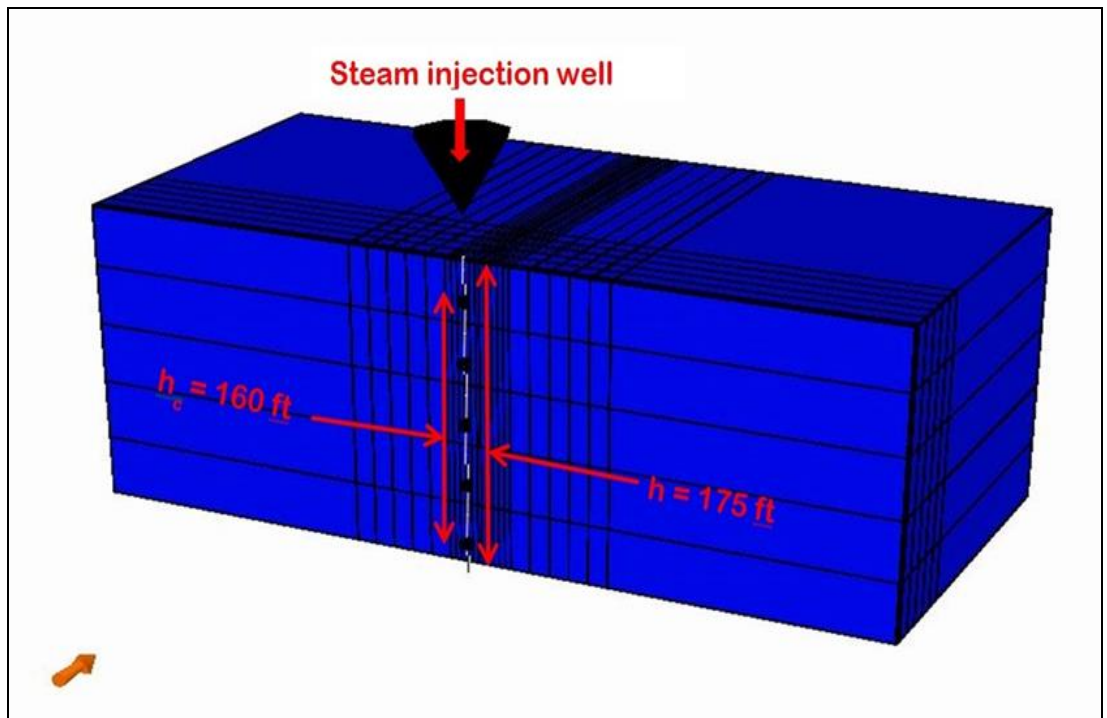


Figure 3.9 : 3D view of displaying open intervals of the injection well.

Table 3.1 : Reservoir and fluid parameters for vertical well.

| | |
|--|----------------------|
| Initial reservoir pressure, psia | 700 |
| Initial reservoir temperature, °F | 93 |
| Porosity, fraction | 0.35 |
| Initial water saturation, % PV | 51 |
| Initial oil saturation, % PV | 49 |
| Horizontal absolute permeability, md | 700 |
| Vertical absolute permeability, md | 70 |
| Pore compressibility, psi ⁻¹ | 300×10^{-6} |
| Water compressibility, psi ⁻¹ | 4×10^{-6} |
| Oil compressibility, psi ⁻¹ | 4.7×10^{-6} |
| Formation thickness, ft | 175 |
| Formation volumetric heat capacity, BTU/(ft ³ - °F) | 35 |
| Formation thermal conductivity, BTU/(ft-D-°F) | 24 |
| Oil viscosity at the initial reservoir condition, cp | 2400 |
| Oil density at standard condition, lb/ft ³ | 63.23 |
| Injection steam temperature, °F | 580 |
| Injection steam quality, fractional steam mass | 0.8 |

Table 3.2 : Grid block sizes.

| Model | Grid blocks i×j×k | Well location | Grid block sizes | | |
|-------------|----------------------|------------------|--------------------------------------|--------------------------------------|------|
| | | | i | j | k |
| 3D model | 23×23×5 | (i,j) | 140, 5×10, 5×3, 2, 5×3, 5×10, 140 | 140, 5×10, 5×3, 2, 5×3, 5×10, 140 | 5×35 |

3.6.1 Methodology for estimating swept volume from falloff test data.

The chief factor in heavy oil recovery is heat. The common practice is to inject hot fluids to the reservoir, thus increasing the temperature of the reservoir and decreasing the viscosity of heavy oil. Average values of temperature, gas saturation, water saturation are calculated as volumetric averages at the instant of shut-in in the steam swept zone. These parameters are necessary to read the values of specific enthalpy, viscosity, specific volume and density of water and steam from steam tables.

The diagnostic plot of falloff period clearly shows that the infinite-acting radial flow is followed by pseudosteady state flow as seen Figure 3.10 for 50 days steam

injection and one day shut-in time. During 50 days steam injection, radial flow regime and pseudosteady state regime are progressed as expected, so 50 days injection plot is selected to show how can distinguish regimes and read slope of plots.

Figures 3.10, 3.11 and 3.13 show the log-log plot of derivative pressure behavior, Cartesian plot and semilog plot of pressure behaviors during the shut-in period for 3D model, respectively. As observed in Figure 3.10, before the infinite-acting radial flow regime (flat line), there is not wellbore storage. At the end of the infinite-acting radial flow regime, the inner boundary between the steam zone and the hot water zone begins to affect (unit slope line). By using the slope of Cartesian straight line in equation 3.6, the steam chamber pore volume is calculated. The slope of the semilog straight line and equation 3.13 are used to calculate the effective permeability. Finally, by using wellbore pressure at shut-in time of one hour in equation 3.15 is used to calculate the skin factor.

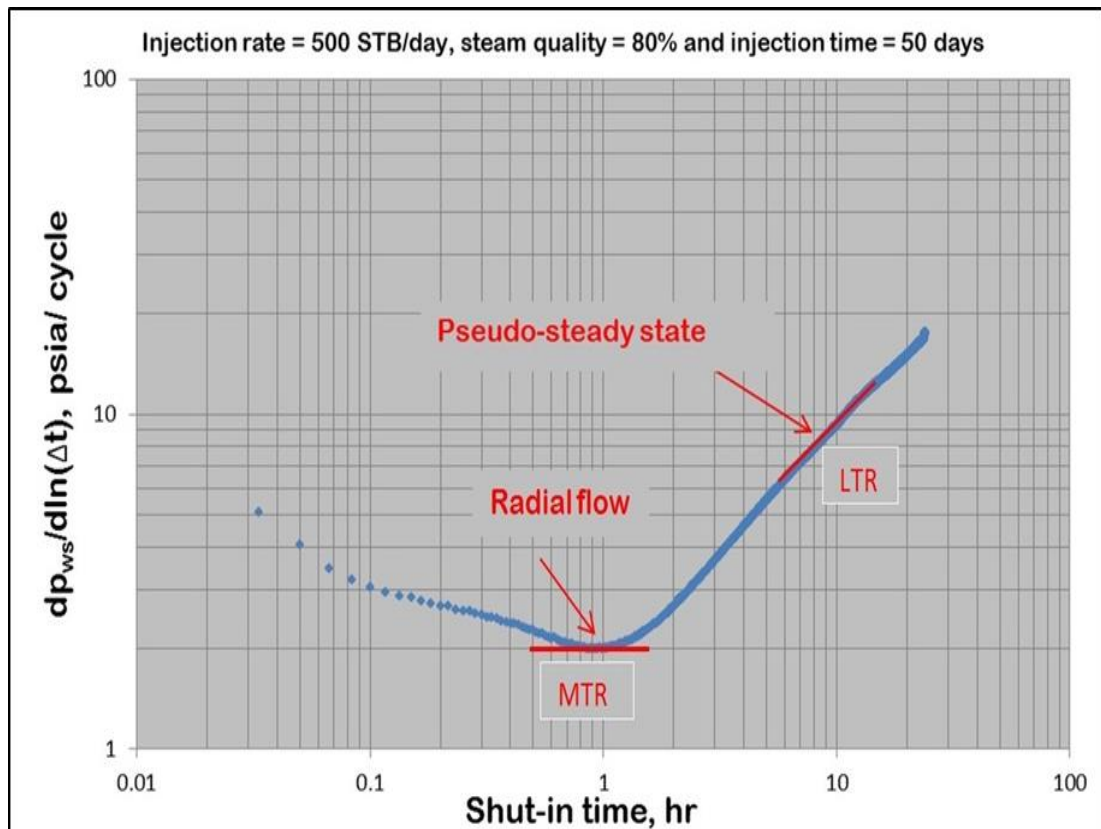


Figure 3.10 : Logarithmic pressure derivative data for 1 day shut-in time after 50 days injection.

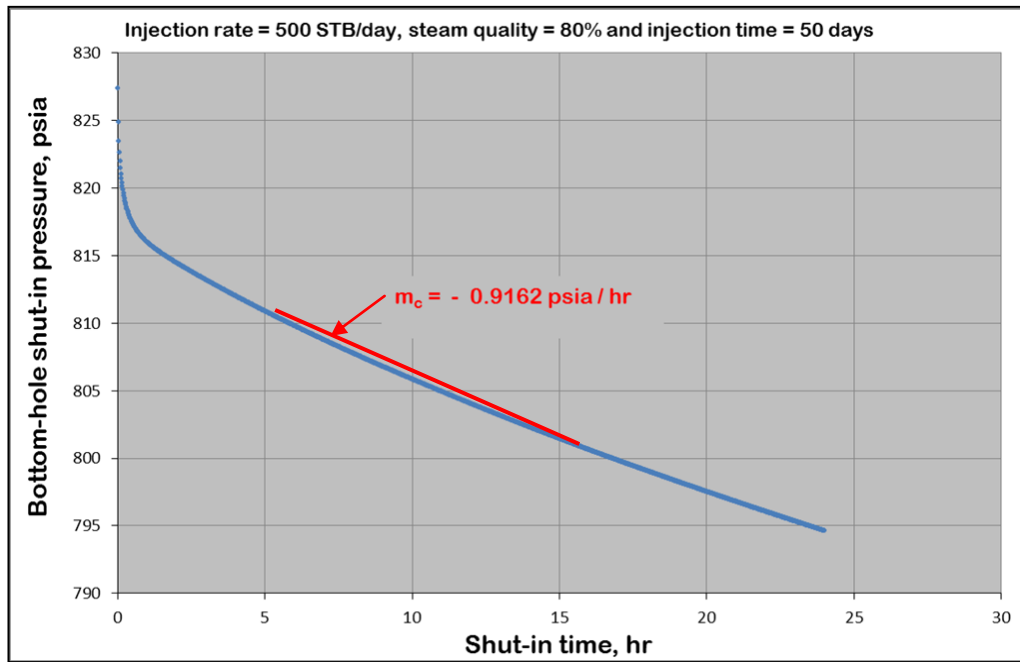


Figure 3.11 : Cartesian pressure data for 1 day shut-in after 50 days injection.

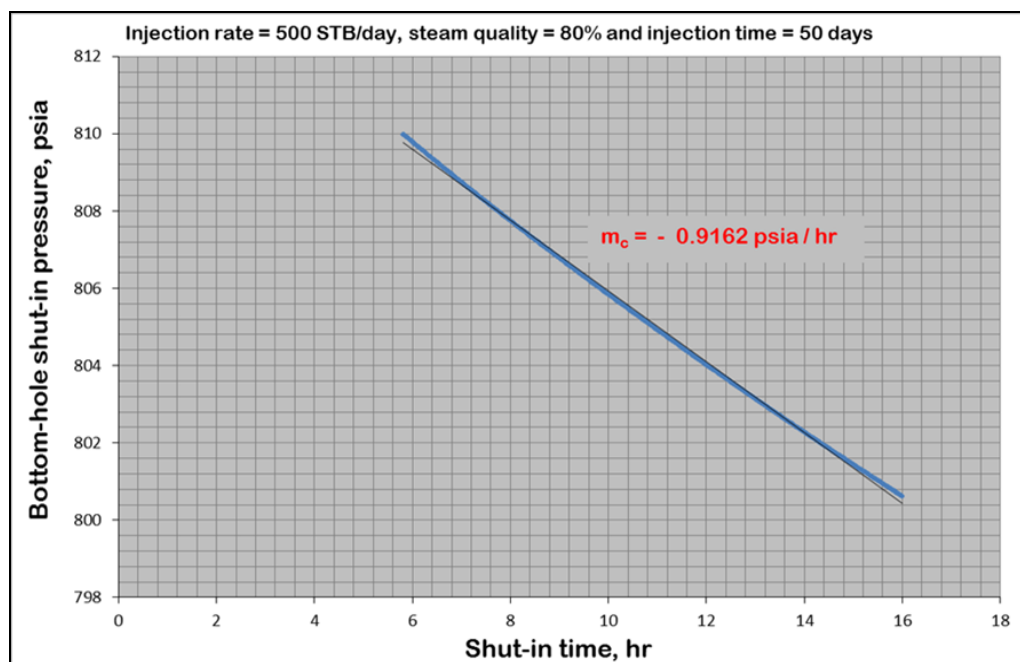


Figure 3.12 : Appearance of Cartesian straight line for 1day shut-in after 50 days injection.

The pressure versus shut-in time yields a Cartesian straight line, according to Figure 3.11 and Figure 3.12, whose slope can be used to calculate the swept volume by equation (3.6):

$$V_s = \frac{q_s B_s}{24 m_c C_t} \quad (3.6)$$

and the steam formation volume factor is given by equation (3.7):

$$B_s = \frac{v_{sv}(T)}{v_{sv}(60^\circ F)} \quad (3.7)$$

where V_s is the swept volume (ft³), q_s is the steam injection rate from the surface, B_s is the volumetric formation factor (res. ft³/std. ft³), m_c is the falloff pressure test pseudosteady state flow slope (dP_{ws}/dt). The value of m_c is obtained by using the MDH pseudosteady state method according to Figures 3.11 and 3.12. C_t is the total compressibility. $v_{sv}(T)$ is specific volume of saturated vapor at steam temperature. $v_{sv}(60^\circ F)$ is specific volume of saturated vapor at 60 °F.

Total compressibility (C_t) is defined in terms of the formation (C_f), water (C_w), oil (C_o), and steam (C_{st}) compressibilities and is given by equation (3.8):

$$C_t = C_f + S_w C_w + S_o C_o + S_{st} C_{st} \quad (3.8)$$

In a SAGD steam injection process, we may not have a single phase, so the concept of the two phase compressibility ($C_{2\phi}$) was used (Shamila et al. 2005). Since the compressibility of steam is much higher than formation, water and oil, C_t is assumed to be equal to the two-phase compressibility ($C_{2\phi}$), equation (3.9): (Grant and Sorey, 1979).

$$C_{2\phi} = (0.18513) \frac{\langle \rho c \rangle}{\phi} \left(\frac{\rho_w - \rho_s}{L_v \rho_w \rho_s} \right)^2 (T + 460) \quad (3.9)$$

where

$$\langle \rho c \rangle = (1 - \phi) \rho_f c_r + \phi S_w \rho_w c_w \quad (3.10)$$

$$c_w = \frac{h_{wT} - h_{wr}}{T - T_r} \quad (3.11)$$

ρc is the volumetric heat capacity (BTU/ft³·°F), L_v is the latent heat of vaporization (BTU/lbm), T is the steam temperature (°F), and ρ_s is the density of the steam injected under reservoir conditions (lbm/ft³). c_r and c_w are rock and water heat capacities respectively with units of BTU/lbm·°F. h_{wT} and h_{wr} are the enthalpy of saturated water at steam temperature and enthalpy of water at reservoir temperature respectively with units (BTU/lbm) (Shamila et al., 2005). The flow rate for steam, q_s is the actual steam injection rate given by equation (3.12):

$$q_s = 5.615q\rho_w f_{st} v_{sv(60^\circ F)} \quad (3.12)$$

q is the steam injection rate from the surface and is known as the Cold Water Equivalent (CWE) and in the units STB/day, ρ_w is the density of water in lbm/ft³, f_{st} is the steam quality (also denoted as f_s) and $v_{sv(60^\circ F)}$ is specific volume saturated vapor at 60 °F.

After the end of wellbore storage effect (if it exists), infinite-acting radial flow occurs. The plot of pressure versus logarithm of shut-in time yields a straight line, according to Figures 3.13 and 3.14. Using the slope of this semilog straight line (m_s), the steam effective permeability and gas phase mobility are calculated from equations (3.13) and (3.14):

$$k_e = \frac{162.6q_s B_s \mu_s}{m_s h} \quad (3.13)$$

$$\lambda_s = \frac{k_e}{\mu_s} \quad (3.14)$$

Using the wellbore pressure at the shut-in time of one hour (p_{1hr}) and equation (3.15), the skin factor can also be calculated:

$$s = 1.1513 \left(\left(\frac{p_{ws} - p_{1hr}}{m_s} \right) - \log \left(\frac{k_e}{\phi \mu_s c_t r_w^2} \right) + 3.23 \right) \quad (3.15)$$

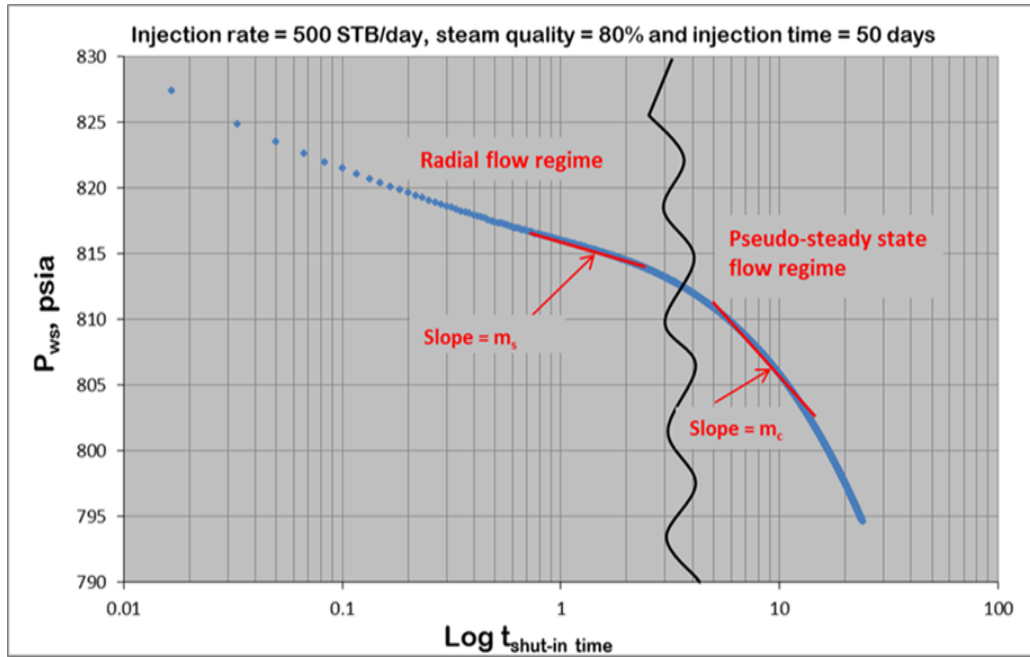


Figure 3.13 : Semilog pressure data for 1 day shut-in after 50 days injection.

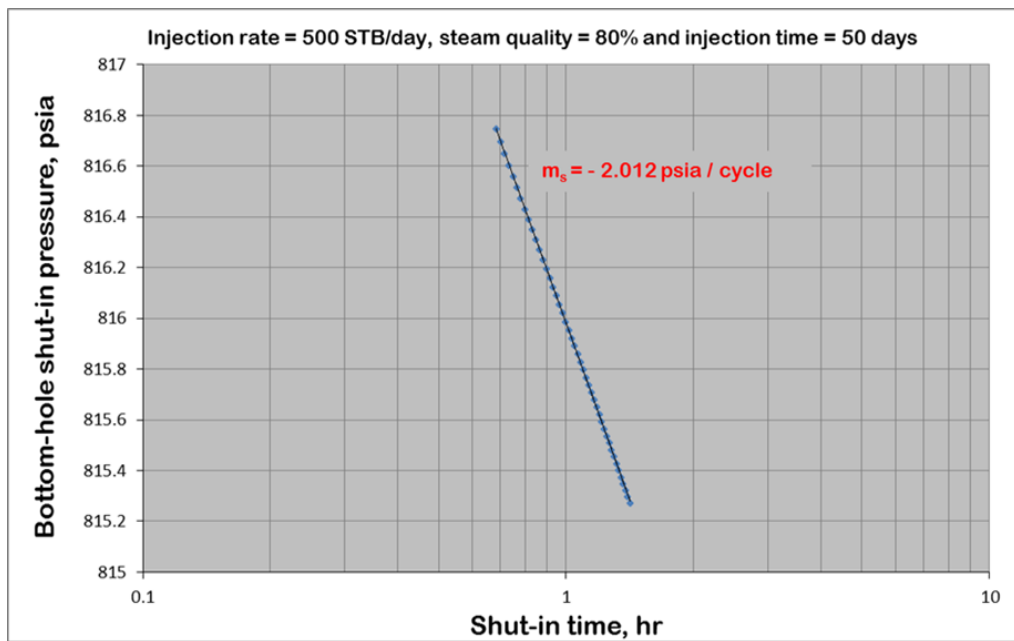


Figure 3.14 : Appearance of semilog straight line for 1day shut-in after 50 days injection.

3.6.2 Estimating swept volume from numerical simulation.

By using the Computer Modelling Group's (CMG) STARS thermal reservoir simulator, reservoir simulations of SAGD are conducted in this procedure. In this simulated system, the volume of the swept steam was estimated automatically by summing the blocks that contain a non-zero gas saturation, because the grid block size was homogeneous in the entire reservoir. The swept volume from a CMG simulation can be estimated by manually summing the blocks that contain non-zero gas saturation volume (Shamila et al., 2005). This gives an accurate estimation of the steam chamber pore volume. The swept pore volume (V_s) for simulations is calculated by using equation (3.16):

$$V_s = (\text{block count}) \times \phi \times (\text{grid block surface area}) \times (\text{lenght of well}) \quad (3.16)$$

4. DISCUSSION OF RESULTS

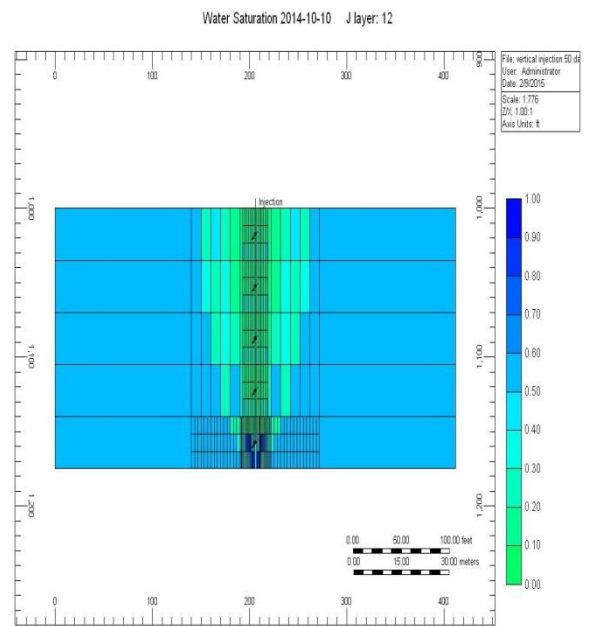
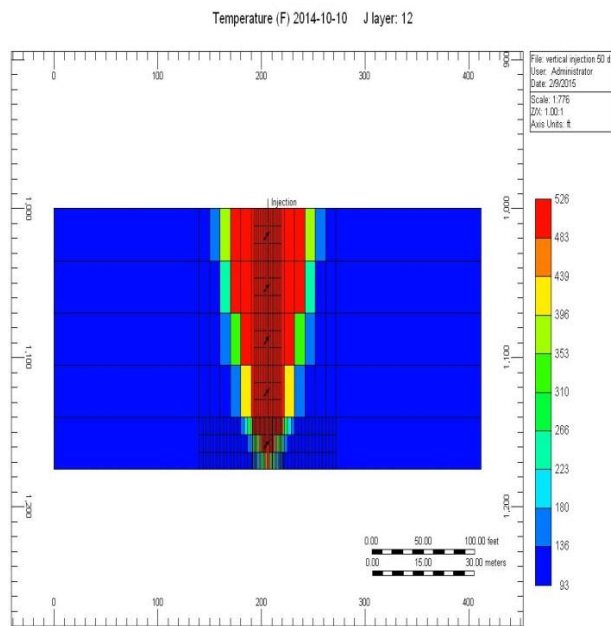
The purpose was to evaluate the accuracy of thermal well testing and to investigate the effects of different parameters on results. Results are compared with the corresponding values obtained from simulation (i.e. permeability at volume weighted average steam saturation within the swept zone and the simulated swept volume).

4.1 Results from Simulator

Reservoir model has five layers and different distributions of temperature, gas saturation and water saturation. Therefore it is needed to calculate volumetric averages to get exact values in each layer. Average values of temperature, gas saturation, water saturation and gas phase mobility are calculated as volumetric averages at the instant of shut-in in the steam swept zone, for 50 days steam injection, 80% steam quality and 500 STB/day. The averages for this particular case are given in Table 4.1. The temperature, water saturation, gas phase mobility, and gas saturation distributions after 50 days steam injection are illustrated in Figure 4.1. For all different cases considered in this study, average values are given in APPENDIX A.1.

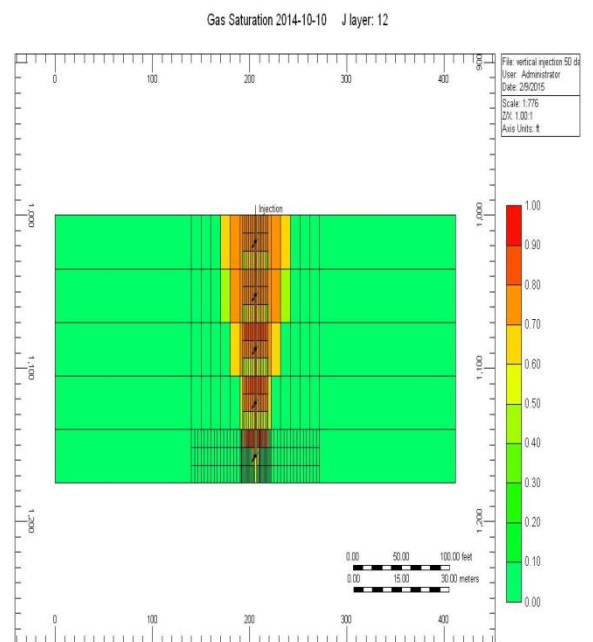
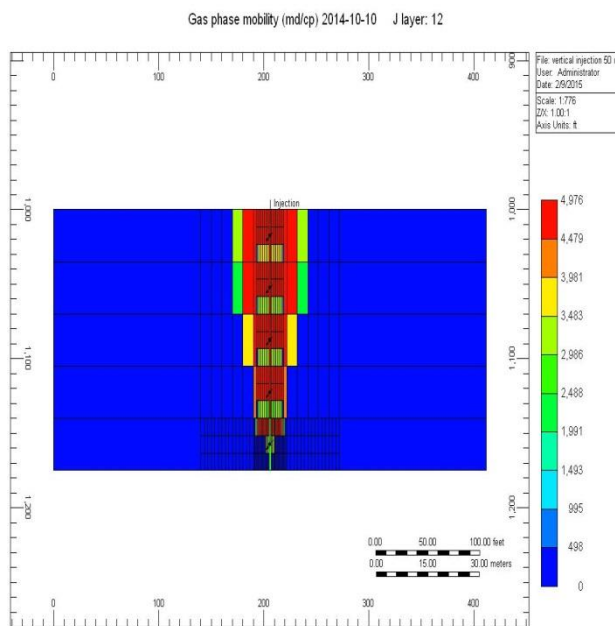
Table 4.1 : Average values of temperature, gas saturation, water saturation and gas phase mobility.

| layers | 1 | 2 | 3 | 4 | 5 | Average |
|-------------|--------|--------|--------|--------|----------|---------|
| λ_s | 4465.7 | 4358.5 | 4445 | 4596.5 | 2453.24 | 4063 |
| Volume | 131040 | 131040 | 94640 | 35840 | 12043.44 | 4377 |
| T | 521 | 521.57 | 522 | 522.44 | 506.12 | 518.6 |
| Volume | 439040 | 296240 | 296240 | 181440 | 57976.56 | 520.9 |
| S_w | 0.234 | 0.242 | 0.26 | 0.293 | 0.528 | 0.31 |
| Volume | 439040 | 439040 | 296240 | 181440 | 57976.56 | 0.26 |
| S_g | 0.741 | 0.724 | 0.739 | 0.757 | 0.483 | 0.68 |
| Volume | 131040 | 131040 | 94640 | 35840 | 12043.44 | 0.73 |



(a)

(b)



(c)

(d)

Figure 4.1 : 50 days steam injection: (a) Temperature, (b) Water saturation, (c) Gas phase mobility, (d) Gas saturation.

4.2 Results from Calculation by Using PSS Method

There is an example of calculation method of swept volume, effective permeability, gas phase mobility and skin factor for 50 days steam injection. At average temperature of 520 °F and average water saturation of 0.26, steam properties are read and used in calculations.

$$\begin{aligned}
 c_w &= \frac{h_{wT} - h_{wr}}{T - T_r} \\
 &= \frac{512 - 61}{520 - 93} = 1.06 \text{ Btu} / \text{lbm} - ^\circ F \\
 c_{2\phi} &= (0.18513) \frac{\leq \rho c >}{\phi} \left(\frac{\rho_w - \rho_s}{L_v \rho_w \rho_s} \right)^2 (T + 460) \\
 &= 0.18513 \times \frac{28}{0.35} \times \left(\frac{47.75 - 1.7996}{685.724 \times 47.75 \times 1.7996} \right)^2 \times (520 + 460) = 0.00872 \text{ psia}^{-1} \\
 \rho c &= (1 - \phi) \rho_f c_r + \phi s_w \rho_w c_w \\
 &= (1 - 0.35) \times 131.1 \times 0.27 + 0.35 \times 0.26 \times 47.75 \times 1.06 = 27.63 \text{ Btu/ft}^3 - ^\circ F \\
 B_s &= \frac{v_{sv(T)}}{v_{sv(^{\circ}60)}} \\
 &= \frac{0.555676}{1205.93} = 0.00046 \\
 q_s &= (q_w f_{st})_{sc} (\rho_w)_{sc} (v_{sv(^{\circ}60)})_{sc} \\
 &= 500 \times 0.8 \times 47.75 \times 1205.93 = 23032298.3 \text{ ft}^3 / \text{day} \\
 m_c &= \frac{777.865 - 775.1}{5.65 - 3.66} = 0.9162 \text{ psia} / \text{hr} \\
 V_{sc} &= \frac{5.615 q_s B_s}{24 m_c \phi c_{2\phi}} \\
 &= \frac{5.615 \times 23032298.3 \times 0.00046}{24 \times 0.9162 \times 0.35 \times 0.00872} = 310957 \text{ ft}^3
 \end{aligned}$$

V_s , steam swept pore volume is 294860 ft³ when is manually calculated from simulator by using equation (3.16). There is a small difference between calculated (PSS method) and simulated values and that is reasonable from practical engineering point of view. The calculated effective permeability to steam and gas phase mobility are determined as follows:

$$k_e = \frac{162.6(q_s)_{sc} B_s \mu_s}{m_s h} = \frac{162.6 \times 23032298.3 \times 0.00046079 \times 0.0183412}{2.012 \times 175} = 89.89 \text{ md}$$

$$\lambda_s = \frac{k_e}{\mu_s} = \frac{89.89}{0.0183412} = 4900 \text{ md / cp}$$

λ_s , gas phase mobility is 4377 md/cp when is manually calculated from simulator by calculation of volumetric averages of five layers of reservoir. There are reasonable differences between calculated and simulated values.

The skin factor can be estimated as follows:

$$\begin{aligned} s &= 1.1513 \left(\left(\frac{p_{ws} - p_{1hr}}{m_s} \right) - \log \left(\frac{k_e}{\phi \mu_s c_t r_w^2} \right) + 3.23 \right) \\ &= 1.1513 \left(\left(\frac{835.57 - 815.98}{2.012} \right) - \log \left(\frac{89.9}{0.35 \times 0.0183412 \times 0.00871533 \times 0.28^2} \right) + 3.23 \right) \\ &= 6.51 \end{aligned}$$

This positive skin factor value is believed to be caused by the partial completion of layers.

4.3 Effect of Injection Time, Injection Rate and Steam Injection Quality on

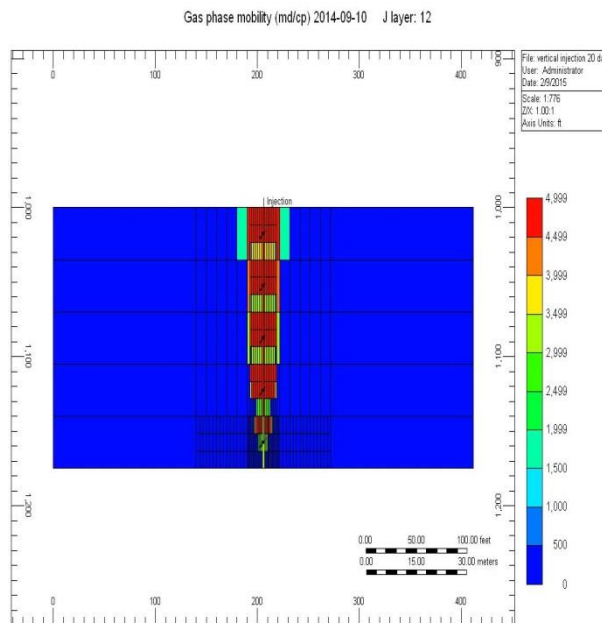
Pressure Behavior

In this study, the effect of injection time, injection rate and steam injection quality on the estimation of steam chamber volume are investigated and comparison between estimation by simulator and PSS method calculation are studied.

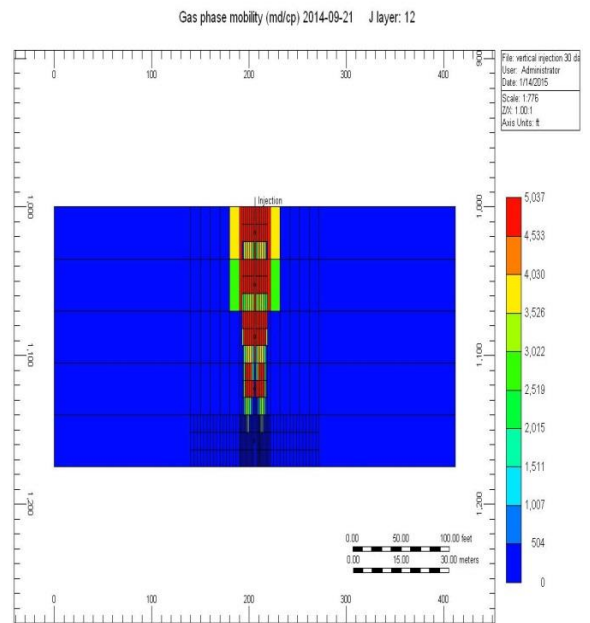
4.3.1 Effect of injection time on steam chamber estimation

To study the effect of steam injection time on the results, different simulation runs with steam injection times of 20, 30, 40 and 50 days are analyzed, respectively. Steam injection rate and steam quality are 500 STB/day and 0.8 and other properties are held constant for these runs. By increasing the time of injection, the volume of steam chamber grows significantly as shown in Figure 4.2. Using simulation for 3D model, the effect of steam injection time was studied. The injection time varies from 20 to 50 days and other properties are kept constant. Steam injection rate and steam

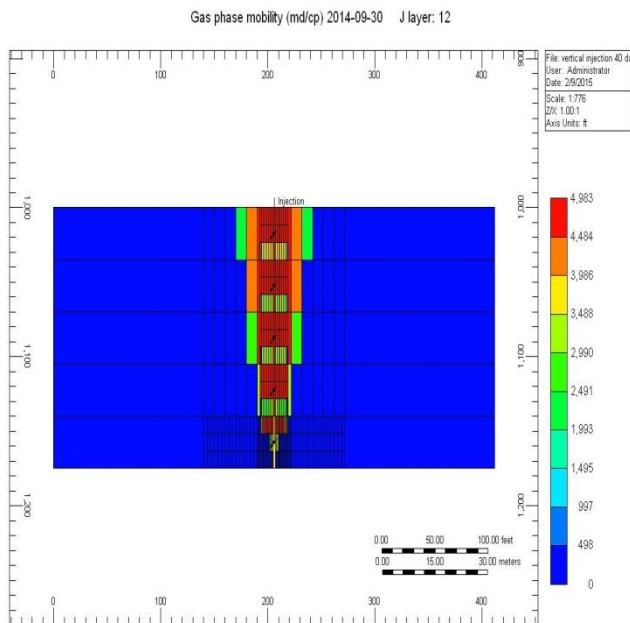
quality are 500 STB/day and 0.8 for these runs. Figure 4.3 shows swept volume as a function of injection time.



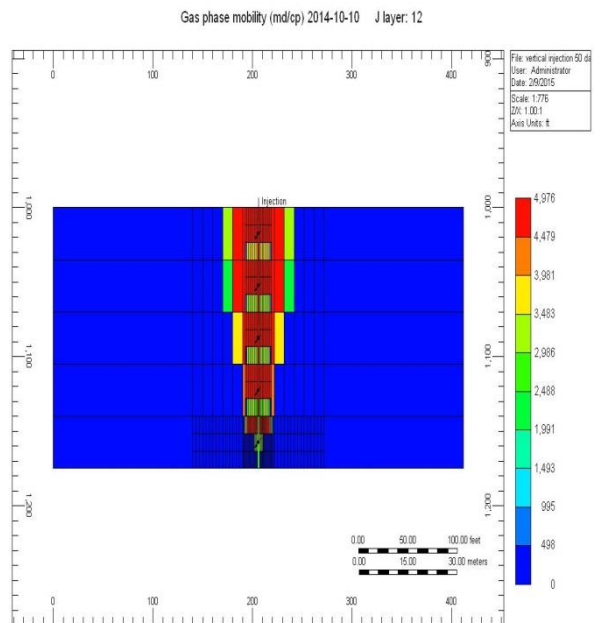
(a)



(b)



(c)



(d)

Figure 4.2 : Steam injection times: (a) 20 days, (b) 30 days, (c) 40 days, (d) 50 days.

For comparing the different flow regimes for various steam injection times, bottom-hole pressure versus time, log-log derivative shut-in pressure versus shut-in time and

Cartesian plot of shut-in pressure versus shut-in time and semilog plot of shut-in pressure versus shut-in time are plotted in Figures 4.4, 4.5, 4.6 and 4.7, respectively.

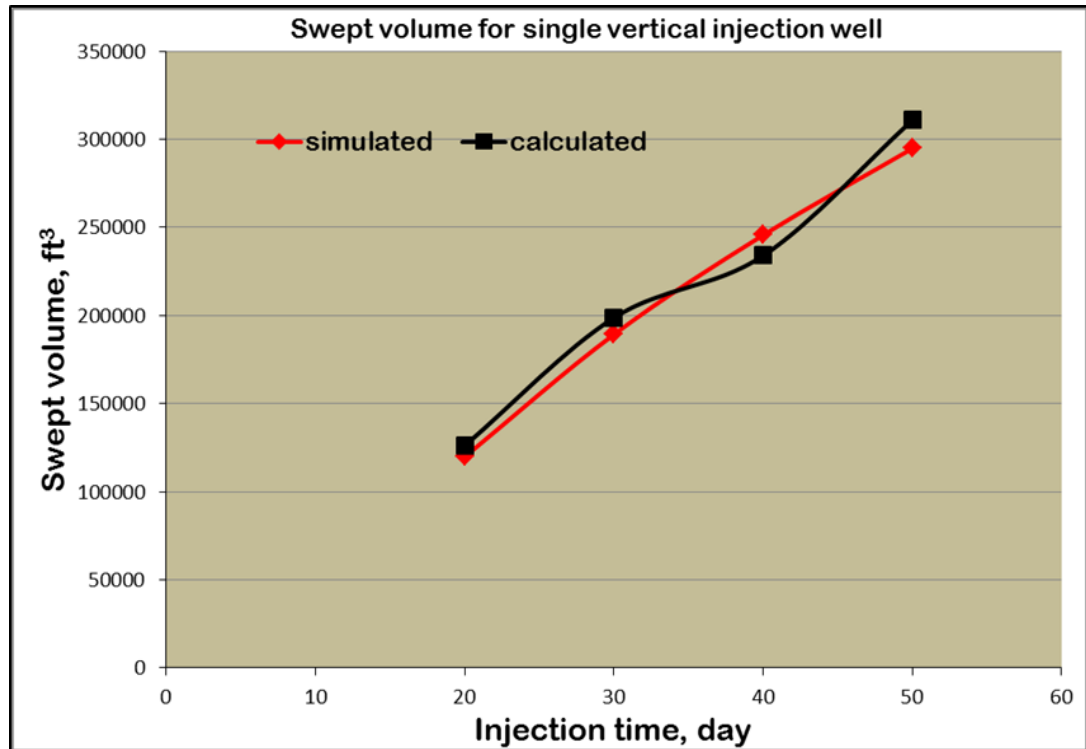


Figure 4.3 : Swept volume changes versus injection times.

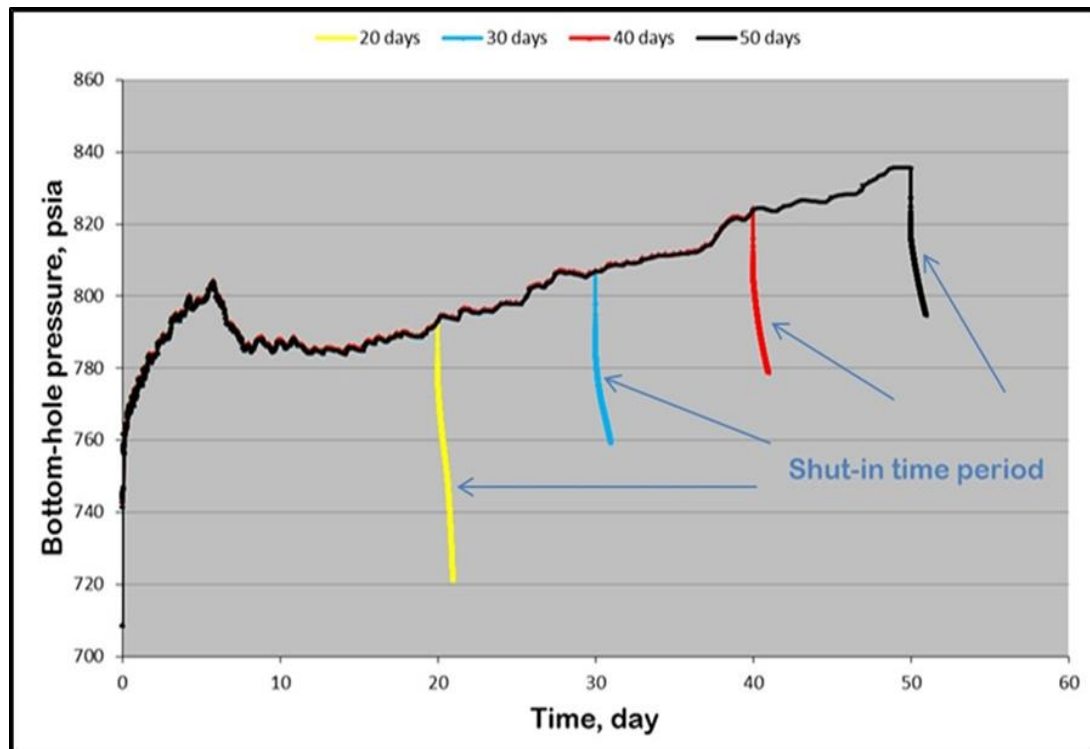


Figure 4.4 : Bottom hole pressures versus various injection times.

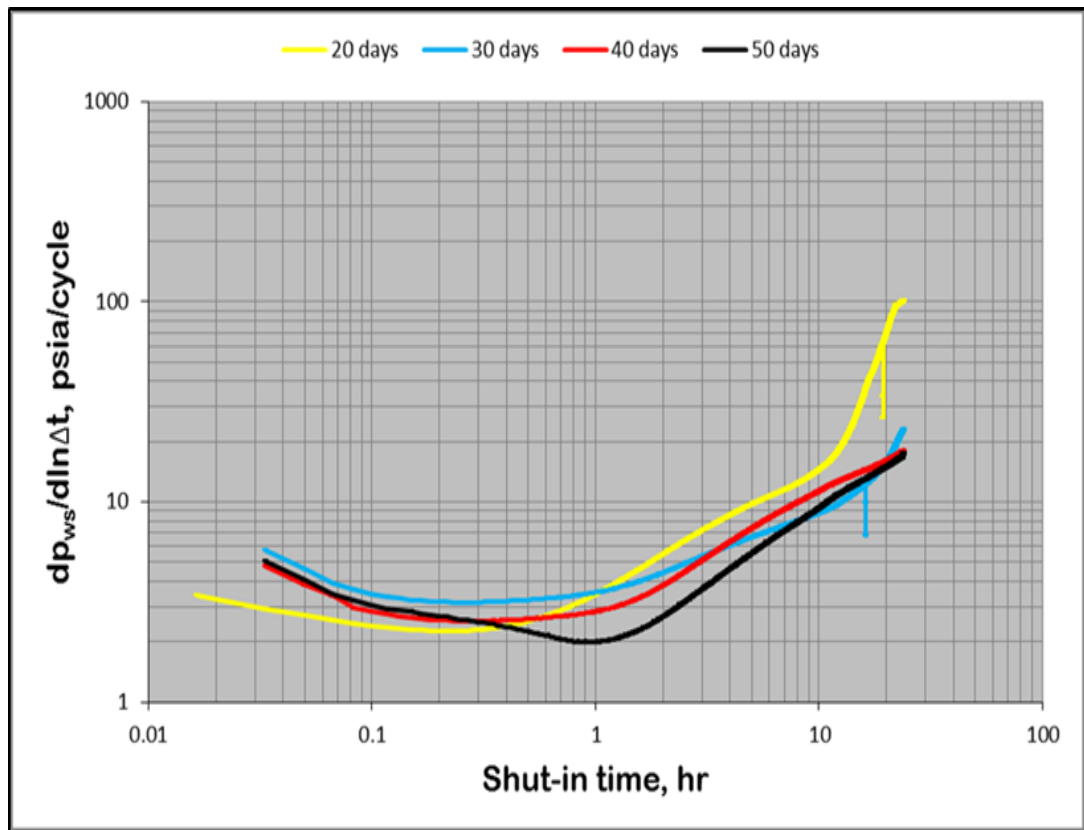


Figure 4.5 : Log-log diagnostic plot of bottom hole shut-in pressure versus shut-in time for various injection time.

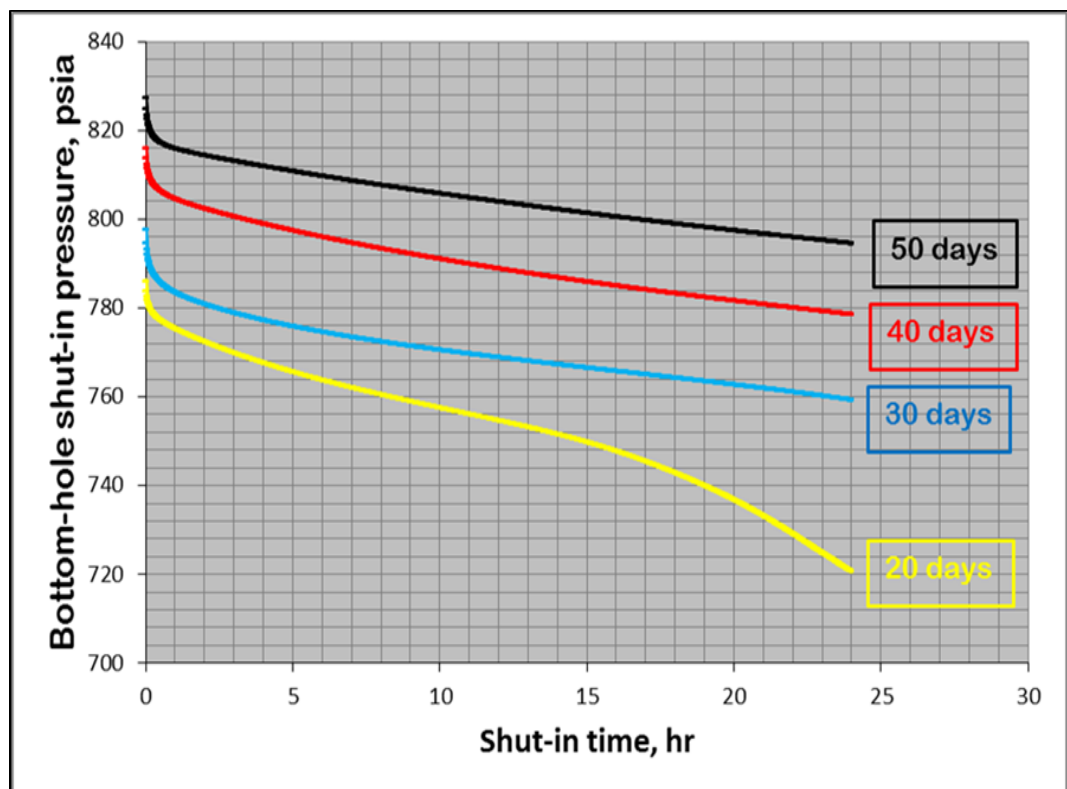


Figure 4.6 : Cartesian plot of bottom hole shut-in pressure versus shut-in time for various injection times.

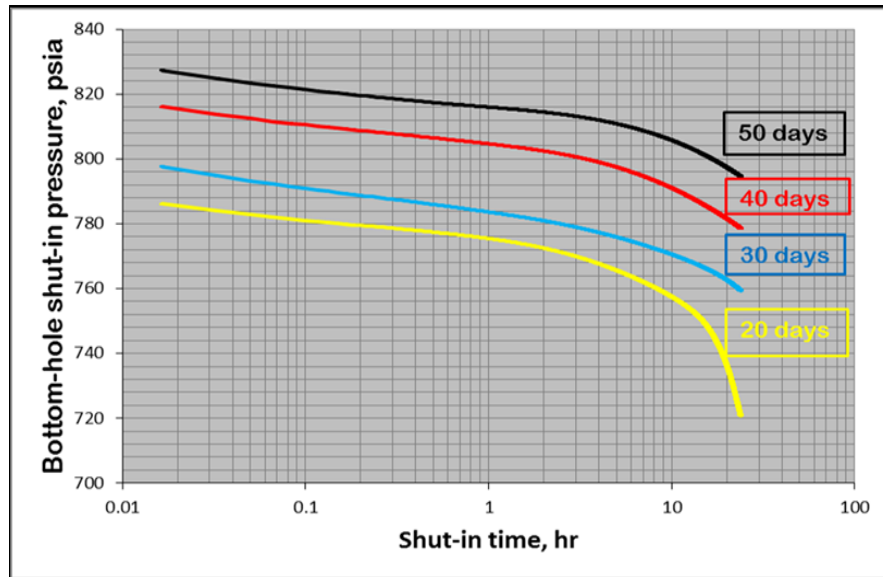


Figure 4.7 : Semilog plot of bottom hole shut-in pressure versus shut-in time for various injection time.

4.3.2 Effect of injection rate on steam chamber estimation

Using simulation for 3D model, the effect of steam injection rate was studied. These runs were conducted with rates 200, 500, 1000 and 1500 STB/day for 30 days steam injection time and holding other properties constant. It is very clear from the swept volume grows significantly between 200 STB/day and 1500 STB/day injection rates in Figure 4.8, but in 500 STB/day injection rate, simulated swept volume value is same as calculated swept volume value. Differences between simulated and calculated values seen reasonable. As expected by increasing steam injection quality, the volume of steam chamber grows. (See Figure A.1 in APPENDIX A.2).

4.3.3 Effect of steam injection quality on steam chamber estimation

Steam quality is designed as the ratio of the steam mass to the total (liquid water and steam) mass injected. The effect of steam injection quality also was studied. These runs were conducted 60%, 70% and 80% steam qualities for 30 days steam injection time with 500 STB/day rate and holding other properties the same. Figure 4.9 gives the comparison of calculated and simulated swept volume effects. Considering the heat balance in the reservoir, the swept volume is expected to increase as the steam quality increase. This fact is clearly observed for the simulated values. At 80% steam quality, the calculated and simulated results match. However the difference between them seems increasing, as the steam quality decreases. At lower steam qualities and

lower injection rates, the swept volumes formed in the reservoir get smaller and thus the PSS period becomes shorter and more difficult to analyze by the Cartesian straight line approach.

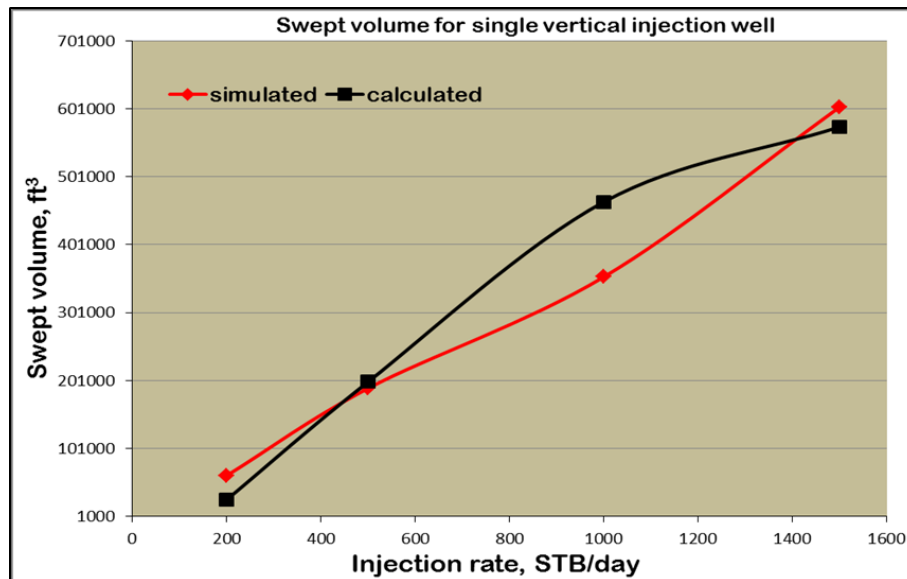


Figure 4.8 : Swept volume changes versus injection rates.

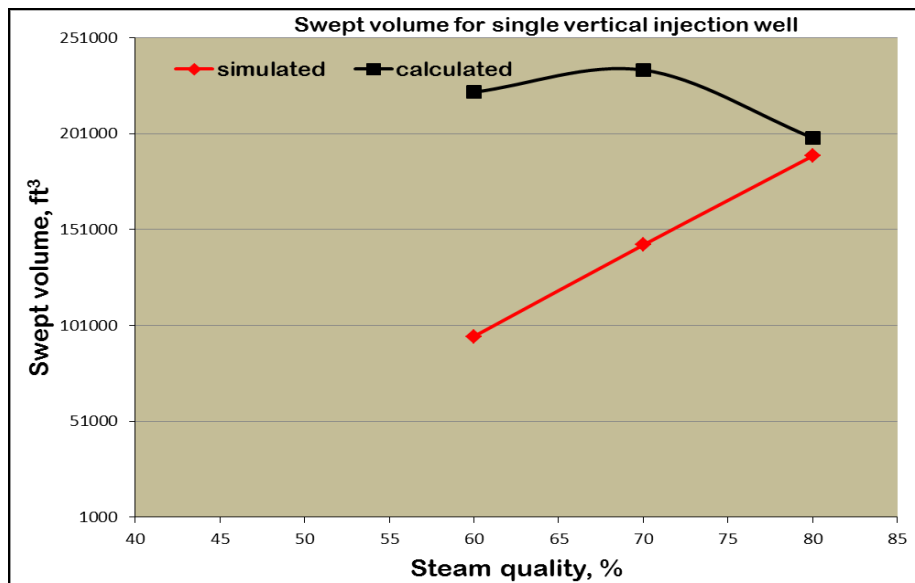


Figure 4.9 : Swept volume changes versus steam injection qualities.

Table 4.2 shows the overall results obtained in this study. The steam chamber volumes calculated from the PSS method and the steam chamber volumes obtained from simulation are in good agreement for various injection times, and for various injection rates. However considerable differences between the calculated and simulated results occur as the steam quality decreases as discussed earlier.

Table 4.2 : Results of the simulated falloff tests and conditions.

| Cases studied | t_i | f_s | q_i | T_{av} (°F) | S_{gav} | S_{wav} | λ_c (md/cp) | λ_s (md/cp) | λ_c/λ_s | V_{sc} (ft ³) | V_s (ft ³) | V_{sc}/V_s |
|------------------------------------|-------|-------|-------|---------------|-----------|-----------|---------------------|---------------------|-----------------------|-----------------------------|--------------------------|--------------|
| Effect of injection time (day) | 20 | 0.8 | 500 | 515 | 0.69 | 0.30 | 4708 | 4117 | 1.14 | 126257 | 119928 | 1.05 |
| | 30 | 0.8 | 500 | 517 | 0.73 | 0.28 | 3359 | 4387 | 0.77 | 198824 | 189384 | 1.05 |
| | 40 | 0.8 | 500 | 519 | 0.73 | 0.27 | 4010 | 4379 | 0.92 | 234033 | 245736 | 0.95 |
| | 50 | 0.8 | 500 | 521 | 0.73 | 0.26 | 4693 | 4378 | 1.07 | 310958 | 294860 | 1.05 |
| Effect of injection rate (STB/day) | 30 | 0.8 | 200 | 498 | 0.73 | 0.33 | 3732 | 4430 | 0.84 | 25243 | 60737 | 0.42 |
| | 30 | 0.8 | 500 | 517 | 0.73 | 0.28 | 3359 | 4387 | 0.77 | 198824 | 189384 | 1.05 |
| | 30 | 0.8 | 1000 | 527 | 0.74 | 0.25 | 4355 | 4427 | 0.98 | 463979 | 353456 | 1.31 |
| | 30 | 0.8 | 1500 | 536 | 0.73 | 0.23 | 4975 | 4308 | 1.15 | 574404 | 603717 | 0.95 |
| Effect of steam injection quality | 30 | 0.6 | 500 | 513 | 0.59 | 0.33 | 2701 | 3167 | 0.85 | 222610 | 95284 | 2.34 |
| | 30 | 0.7 | 500 | 515 | 0.65 | 0.30 | 3037 | 3684 | 0.82 | 234174 | 142948 | 1.64 |
| | 30 | 0.8 | 500 | 517 | 0.73 | 0.28 | 3359 | 4387 | 0.77 | 198824 | 189384 | 1.05 |

V_{sc} : Steam chamber volume calculated.

V_s : Steam chamber volume from simulator.

λ_c : Gas phase mobility calculated.

λ_s : Gas phase mobility from simulator.

T_{av} : Average temperature in steam chamber.

S_{gav} : Average gas saturation in steam chamber.

S_{wav} : Average water saturation in steam chamber.

5. CONCLUSIONS

In this study, the thermal well test analysis using the pseudo steady state method proposed by Satman et al. (1980) is investigated for steam chamber volume estimations. The falloff pressure data are obtained from the STARS simulator. We studied to understand the effects of the injection time, injection rate and the steam quality on estimation of the steam chamber volume.

Thermal well test analysis discussed in this study consists of a falloff (shut-in) period following an injection period. The reservoir is treated as having two zones around the injection well. The zone around the injection well represents the steam chamber volume. This creates a mobility discontinuity between the steam chamber zone where steam predominates and the region where the original reservoir fluids predominates. Falloff testing is used in such systems to determine the steam zone volume. The slope of the first part of a falloff test develops on a standard plot of pressure versus logarithm of time is used to estimation the permeability of the steam zone. The slope of the pseudo steady state behavior beyond the semilog straight line is used to estimate the steam zone volume.

As discussed in this thesis, the pseudo steady state behavior is affected by the injection time, the injection rate and the steam quality. For the cases studied the calculated steam chamber volume and the permeabilities of the steam zone obtained from falloff analysis are generally in reasonable agreements with the results obtained from the simulator. As the results indicate the difference between the calculated and the simulator becomes significant if the injection rate and the steam quality become lower. This is an expected result since the occurrence of the steam chamber zone is affected by the heat transfer mechanisms between the steam chamber and the over-lying and under-lying formations and cause smaller steam chamber zones and shorter pseudo steady state periods.

At low injection rates and small steam injection qualities, radial flow regime and pseudo steady state are not progressed due to relatively high heat losses to over- and under-burden formations, and increasing effects of two phase (steam+hot water) flow

in steam zone, so this causes errors in reading slopes and interpretation results in Cartesian and semilog plots. As the injection rate increases, the accuracy of volume estimation gets better. At higher rates, the radial flow representing the steam swept zone becomes clear and a second radial flow representing the unswept zone may be observed in some cases. As the injection rate increases, the estimated permeability values get closer to the simulated values.

Better estimates of swept volume seem to be obtained as the steam quality increases. Injection with higher steam quality leads to formation of a larger steam chamber and thus a longer period of pseudosteady state pressure.

In general, the pseudosteady period occurs in durations from a fraction of an hour to a few hours.

REFERENCES

- Akhondzadeh, H., Fattahi, A.** (2014). Impact of Well Configuration on Performance of Steam-based Gravity Drainage Processes in Naturally Fractured Reservoirs. *Journal of Petroleum Exploration and Production Technology*, Vol. 5, Issue 1, 13-25.
- Akin, S.** (2005). Mathematical Modeling of Steam-Assisted Gravity Drainage. SPE 86963.
- Banerjee, D.K.** (2012). Oil Sands, Heavy Oil and Bitumen from Recovery to Refinery. Vol. 5, Penn Well Corporation. Tulsa, Oklahoma, USA.
- Butler, R.M.** (1982). Method for Continuously Producing Viscous Hydrocarbons by Gravity Drainage while Injecting Heated Fluids. US Patent No. 4344485.
- Butler, R.M.** (1991). Thermal Recovery of Oil and Bitumen. Prentice Hall. Michigan, USA.
- Butler, R.M., Dargie, B.** (1994). Horizontal Wells for the Recovery of Oil, Gas and Bitumen, Petroleum Society Monograph, No. 2, Alberta, Canada.
- Butler, R.M., Jiang, Q., Yee, C.T.** (2001). The Steam and Gas Push (SAGP)-4; Recent Theoretical Developments and Laboratory Results Using Layered Models. PETSOC-01-01-06.
- Coats, K.H., George, W.D., Marcum, B.E.** (1974). Three Dimensional Simulation of Steamflooding. SPE-4500-PA.
- Chen, Q., Gerritsen, M.G., Kovscek, A.R.** (2008). Effects of Reservoir Heterogeneities on the Gravity Drainage Process. SPE-109873-PA.
- CMG (STARS).** (2012). User Manual. Computer Modelling Group. Calgary, Alberta.
- Edmunds, N.R., Gittins, S.D.** (1993). Effective Application of Steam Assisted Gravity Drainage of Bitumen to Long Horizontal Well Pairs. PETSOC-93-06-05
- Edmunds, N.R., Kovalsky, J.A., Gittins, S.D., Pennacchioli, E.D.** (1994). Review of Phase Steam-Assisted Gravity Drainage Test. SPE-21529-PA.
- Eggenschwiler, M., Satman, A., Ramey, H.r.** (1980). Interpretation of Injection Well Pressure Transient Data in Thermal Oil Recovery. SPE 8908.
- Farouq Ali, S.M.** (1997). Is There Life After SAGD? PETSOC-97-06-DAS.
- Gates, I.D., Leskiw, C.** (2008). Impact of Steam Trap Control on Performance of Steam-Assisted Gravity Drainage, PETSOC-2008-112-EA.

- Grant, M.A., Sorey, M.L.** (1979). The Compressibility and Hydraulic Diffusivity of a Water-Steam Flow. *Water Resources Research* Vol. 15, No. 3, 684-86.
- Issaka, M.B., Ambastha, A.K.** (1992). Thermal Well Testing for a Horizontal Well. PETSOC-92-24
- Jahanbani, G.A., Jelmert, T.A., Kleppe, J.** (2011). Simulation Study of Thermal Well Test Analysis in Steam Injection Wells. SPE 150295.
- Jahanbani, G.A., Jelmert, T.A., Kleppe, J., Ashrafi, M., Souraki, Y., Toresaeter, O.** (2012a). Investigation of Applicability of Thermal Well Test Analysis in Steam Injection Wells for Athabasca Heavy Oil. SPE 154182
- Jahanbani, G.A., Jelmert, T.A., Kleppe, J.** (2012b). Investigation of Thermal Well Test Analysis for Horizontal Wells in SAGD Process. SPE 159680
- Kazemi, H.** (1966). Locating a Burning Front by Pressure Transient Measurements. *Journal of Petroleum Technology*, Vol. 18, Issue 02, 227-232.
- Khan, M.A.B., Mehrotra, A.K. Svrcek, W.Y.** (1984). Viscosity Models for Gas-Free Athabasca Bitumen. PETSOC-84-03-05
- Lee, J.** (1982). Well Testing. SPE Textbook Series. Vol. 1. Dallas.
- Levitan, M.M., Clay, P.L., Gilchrist, J.M.** (2001). How Good Are Your Horizontal Wells? SPE-68943-MS.
- Mehrotra, A.K. Svrcek, W.Y.** (1986). Correlations for Properties of Bitumen Saturated with CO₂, CH₄ and N₂, and Experiments with Combustion Gas Mixtures. *Journal of Canadian Petroleum Technology*., Vol. 21, Issue 06, 95-104.
- Nasr, T.N., Ayodele, O.R.** (2005). Thermal Techniques for the Recovery of Heavy Oil and Bitumen. SPE 97488.
- O'Rourke, J.C., Chambers, J.I., Suggett, J.C., Good, W.K.** (1994). UTF Project Status and Commercial Potential an Update, May 1994, 94-40, Calgary, Alberta.
- Peaceman, P.W.** (1983). Interpretation of Well-block Pressure in Numerical Reservoir Simulation with Nonsquare Gridblocks and Anisotropic Permeability. SPE 10528-PA.
- Polikar, M., Farouq Ali, S., Puttagunta, V.** (1990). High-Temperature Relative Permeabilities for Athabasca Oil Sands. SPE 17424-PA.
- Sahuquet, B.C., Spreux, A.M., Corre, B., Guittard, M.P.** (1990). Steam in a Low-Permeability Reservoir Through a Horizontal Well in Lacq Superieur Field. SPE-20526-MS.
- Satman, A., Eggenschwiler, M., Tang, R. W-K., Ramey, H.J.** (1980). An Analytical Study of Transient Flow in Systems with Radial Discontinuities. SPE 9399.
- Satter, A., Iqbal, G.M., Buchwalter, J.L.** (2008). Practical Enhanced Reservoir Engineering Assisted with Simulation Software. Penn Well Corporation, Tulsa, Oklahoma, USA.

- Sawhney, G.S., Liebe, H., Butler, R.M.** (1995). Vertical Injection Wells for SAGD: A Practical Option or Not? *Journal of Canadian Petroleum Technology*, Vol. 34, Issue 01.
- Sedaei, B., Rashidi, F.** (2006). Application of the SAGD to an Iranian Carbonate Heavy Oil Reservoir. SPE 100533.
- Shamila, A., Shirif, E., Dong, M., Henni, A.** (2005). Chamber Volume/Size Estimation for SAGD Process Horizontal Well Testing. PETSOC-2005-075.
- Sheng, J.J.** (2013). Enhanced Oil Recovery Field Case Studies. Texas Tech University, May, Gulf Professional Publishing, Houston, Texas, USA.
- Shin, H., Polikar, M.** (2005). Optimizing the SAGD Process in Three Major Canadian Oil-Sands Areas, SPE 95754.
- Singhal, A.K., Ito, Y., Kasraie, M.** (1998). Screening and Design Criteria for Steam Assisted Gravity Drainage (SAGD) projects, SPE-50410-MS.
- Speight, J.G.** (2009). Enhanced Recovery Methods for Heavy Oil and Tar Sands. Gulf Publishing Company, Houston, Texas, USA.
- Tarhuni, H., Shirif, E., Ayub, M., Henni, A.** (2004). Theoretical Analysis of Steam Assisted Gravity Drainage Process. PETSOC-2004-057.
- Url-1** <<http://www.surmontenergy.com/operations>>, date retrieved 20.08.2014.
- Url-2** <<http://www.energy.gov.ab.ca/oilsands/793.asp>>, date retrieved 20.08.2014.
- Url-3** <<http://blog.cdnoilsands.com/figuring-out-the-oil-sands-part-1>>, date retrieved 20.08.2014.
- Url-4**<<http://laricinaenergy.com/uploads/tech/GPS%20Bitumen%20Mobilization.pdf>>, date retrieved 20.08.2014.
- Url-5**<<http://laricinaenergy.com/operations/saleski.html>>, date retrieved 20.08.2014.
- Url-6**<http://en.wikipedia.org/wiki/Karl_Clark_%28chemist%29>, date retrieved 20.08.2014.
- Url-7** <<http://glcm.cee.illinois.edu/node/112>>, date retrieved 24.04.2015.
- Url-8** <<http://large.stanford.edu/courses/2010/ph240/alnoaimi1/>>, date retrieved 20.08.2014.
- Wong, R.C.K., Li, Y., Yeung, K.C.** (1999). Analysis of Well Testing in an Oil Sand Reservoir. PETSOC-99-30.
- Yee, C.T., Stroich, A.** (2004). Flue Gas Injection into a Mature SAGD Steam Chamber at the Dover Project (Formerly UTF). PETSOC-04-01-06.
- Zamani, A., James, B.R., Hite, R.R.** (2013). Use of Pressure Transient Analysis for Monitoring SAGD Steam Chamber Development. SPE-165489-MS.

APPENDICES

APPENDIX A.1 : Tabulated Results of the Effects of Steam Injection Time, Injection Rate and Steam Injection Quality.

APPENDIX A.2 : Graphical Results Obtained from Simulator for Steam Injection Rates and Steam Injection Quality Variations.

APPENDIX A.1: Tabulated Results of the Effects of Steam Injection Time, Injection Rate and Steam Injection Quality.

Table A.1 : Average values of temperature, gas saturation, water saturation and gas phase mobility for various steam injection times.

| | | | | | | |
|----------------|--------|---------|--------|--------|----------|----------|
| 20 days | | | | | | |
| Layers | 1 | 2 | 3 | 4 | 5 | Average |
| λ_s | 4314.6 | 4534.7 | 4396.5 | 4511 | 2813 | 4113.96 |
| volume | 38640 | 35840 | 35840 | 35840 | 35840 | 4117.047 |
| T | 515.17 | 515.25 | 515.7 | 516 | 503.6 | 513.144 |
| volume | 181440 | 181440 | 94640 | 94640 | 26187.48 | 514.8938 |
| S_w | 0.28 | 0.289 | 0.292 | 0.311 | 0.495 | 0.3334 |
| volume | 296240 | 181440 | 181440 | 94640 | 36050 | 0.298352 |
| S_g | 0.714 | 0.747 | 0.731 | 0.745 | 0.53 | 0.6934 |
| volume | 38640 | 35840 | 35840 | 35840 | 35840 | 0.693717 |
| 30 days | | | | | | |
| layers | 1 | 2 | 3 | 4 | 5 | Average |
| λ_s | 4519.5 | 4446.7 | 4474.6 | 4470.5 | 2356 | 4053.46 |
| volume | 94640 | 94640 | 35840 | 35840 | 12039.44 | 4386.524 |
| T | 516.65 | 517.73 | 517.77 | 518.36 | 500.9 | 514.282 |
| volume | 296240 | 181440 | 181440 | 94640 | 36260.12 | 516.6372 |
| S_w | 0.26 | 0.263 | 0.292 | 0.295 | 0.511 | 0.3242 |
| volume | 296240 | 296240 | 181440 | 181440 | 36260.12 | 0.282334 |
| S_g | 0.745 | 0.737 | 0.741 | 0.738 | 0.465 | 0.6852 |
| volume | 94640 | 94640 | 35840 | 35840 | 12039.44 | 0.728434 |
| 40 days | | | | | | |
| layers | 1 | 2 | 3 | 4 | 5 | Average |
| λ_s | 4353.5 | 4543.15 | 4342.9 | 4510 | 3197.45 | 4189.4 |
| volume | 100240 | 94640 | 94640 | 35840 | 11950 | 4379.409 |
| T | 519.5 | 519.8 | 520.5 | 520.7 | 507.5 | 517.6 |
| volume | 296240 | 296240 | 181440 | 94640 | 46493.28 | 519.3098 |
| S_w | 0.243 | 0.26 | 0.27 | 0.29 | 0.518 | 0.3162 |
| volume | 439040 | 296240 | 296240 | 181440 | 37940.6 | 0.268578 |
| S_g | 0.723 | 0.75 | 0.724 | 0.746 | 0.588 | 0.7062 |
| volume | 100240 | 94640 | 94640 | 35840 | 11950 | 0.728517 |
| 50 days | | | | | | |
| layers | 1 | 2 | 3 | 4 | 5 | Average |
| λ_s | 4465.7 | 4358.5 | 4445 | 4596.5 | 2453.24 | 4063.788 |
| volume | 131040 | 131040 | 94640 | 35840 | 12043.44 | 4377.822 |
| T | 521 | 521.57 | 522 | 522.44 | 506.12 | 518.626 |
| volume | 439040 | 296240 | 296240 | 181440 | 57976.56 | 520.8927 |
| S_w | 0.234 | 0.242 | 0.26 | 0.293 | 0.528 | 0.3114 |
| volume | 439040 | 439040 | 296240 | 181440 | 57976.56 | 0.261561 |
| S_g | 0.741 | 0.724 | 0.739 | 0.757 | 0.483 | 0.6888 |
| volume | 131040 | 131040 | 94640 | 35840 | 12043.44 | 0.728764 |

Table A.2 : Average values of temperature, gas saturation, water saturation and gas phase mobility for various steam injection rates.

| | | | | | | |
|----------------------|--------|--------|----------|---------|----------|----------|
| 200 STB/ day | | | | | | |
| layers | 1 | 2 | 3 | 4 | 5 | Average |
| λ_s | 4559.2 | 4569.5 | 3580.5 | 0 | 0 | 4236.4 |
| volume | 35840 | 35840 | 11308.23 | 0 | 0 | 4430.288 |
| T | 510 | 510.8 | 498.71 | 204 | 94 | 363.502 |
| volume | 94640 | 94640 | 35840 | 7888.92 | 0 | 498.2282 |
| S_w | 0.29 | 0.29 | 0.46 | 0.52 | 0.511 | 0.4142 |
| volume | 181440 | 181440 | 94640 | 11950 | 140 | 0.330179 |
| S_g | 0.747 | 0.747 | 0.636 | 0 | 0 | 0.71 |
| volume | 35840 | 35840 | 11308.23 | 0 | 0 | 0.731875 |
| 500 STB/ day | | | | | | |
| layers | 1 | 2 | 3 | 4 | 5 | Average |
| λ_s | 4519.5 | 4446.7 | 4474.6 | 4470.5 | 2356 | 4053.46 |
| volume | 94640 | 94640 | 35840 | 35840 | 12039.44 | 4386.524 |
| T | 516.65 | 517.73 | 517.77 | 518.36 | 500.9 | 514.282 |
| volume | 296240 | 181440 | 181440 | 94640 | 36260.12 | 516.6372 |
| S_w | 0.26 | 0.263 | 0.292 | 0.295 | 0.511 | 0.3242 |
| volume | 296240 | 296240 | 181440 | 181440 | 36260.12 | 0.282334 |
| S_g | 0.745 | 0.737 | 0.741 | 0.738 | 0.465 | 0.6852 |
| volume | 94640 | 94640 | 35840 | 35840 | 12039.44 | 0.728434 |
| 1000 STB/ day | | | | | | |
| layers | 1 | 2 | 3 | 4 | 5 | Average |
| λ_s | 4394 | 4419.9 | 4504 | 4451.66 | 4308 | 4415.512 |
| volume | 125440 | 125440 | 94640 | 94640 | 37730.54 | 4427.211 |
| T | 526 | 526.7 | 527.2 | 527.44 | 528 | 527.068 |
| volume | 439040 | 439040 | 296240 | 296240 | 101948.8 | 526.8224 |
| S_w | 0.237 | 0.23 | 0.266 | 0.26 | 0.32 | 0.2626 |
| volume | 609840 | 439040 | 439040 | 296240 | 121835 | 0.250948 |
| S_g | 0.735 | 0.739 | 0.749 | 0.743 | 0.725 | 0.7382 |
| volume | 125440 | 125440 | 94640 | 94640 | 37730.54 | 0.739617 |
| 1500 STB/ day | | | | | | |
| layers | 1 | 2 | 3 | 4 | 5 | Average |
| λ_s | 4219.2 | 4281.7 | 4390 | 4363.3 | 4266.1 | 4304.06 |
| volume | 184240 | 184240 | 181440 | 181440 | 95480.24 | 4307.643 |
| T | 535.8 | 536.67 | 534.1 | 537.18 | 537.4 | 536.23 |
| volume | 439040 | 439040 | 439040 | 439040 | 181440 | 536.0745 |
| S_w | 0.22 | 0.214 | 0.241 | 0.237 | 0.308 | 0.244 |
| volume | 609840 | 609840 | 609840 | 609840 | 212940 | 0.234423 |
| S_g | 0.72 | 0.726 | 0.74 | 0.737 | 0.726 | 0.7298 |
| volume | 184240 | 184240 | 181440 | 181440 | 95480.24 | 0.730149 |

Table A.3 : Average values of temperature, gas saturation, water saturation and gas phase mobility for various steam injection qualities.

| | | | | | | |
|---------------|---------------|---------------|---------------|---------------|--------------|----------------|
| 60% | | | | | | |
| Layers | 1 | 2 | 3 | 4 | 5 | Average |
| λ_s | 3214.3 | 3223.2 | 3187.81 | 3197.13 | 285 | 2621.488 |
| volume | 63840 | 35840 | 35840 | 24296.94 | 2287.32 | 3166.5045 |
| T | 515.45 | 514.95 | 516.75 | 517.3 | 438 | 500.49 |
| volume | 296240 | 181440 | 94640 | 94640 | 21931.55 | 513.28536 |
| S_w | 0.293 | 0.33 | 0.32 | 0.35 | 0.553 | 0.3692 |
| volume | 296240 | 296240 | 181440 | 94640 | 35840 | 0.3268043 |
| S_g | 0.595 | 0.596 | 0.592 | 0.593 | 0.137 | 0.5026 |
| volume | 63840 | 35840 | 35840 | 24296.94 | 2287.32 | 0.5877956 |
| 70% | | | | | | |
| Layers | 1 | 2 | 3 | 4 | 5 | Average |
| λ_s | 3774.08 | 3702.3 | 3704.76 | 3624 | 2340.7 | 3429.168 |
| volume | 72240 | 72240 | 35840 | 35840 | 4761.36 | 3684.1226 |
| T | 516.52 | 517.65 | 517.67 | 518.3 | 473 | 508.628 |
| volume | 296240 | 181440 | 181440 | 94640 | 35840 | 515.28189 |
| S_w | 0.28 | 0.284 | 0.305 | 0.318 | 0.552 | 0.3478 |
| volume | 296240 | 296240 | 181440 | 181440 | 35840 | 0.3025627 |
| S_g | 0.66 | 0.65 | 0.653 | 0.635 | 0.452 | 0.61 |
| volume | 72240 | 72240 | 35840 | 35840 | 4761.36 | 0.6470558 |
| 80% | | | | | | |
| layers | 1 | 2 | 3 | 4 | 5 | Average |
| λ_s | 4519.5 | 4446.7 | 4474.6 | 4470.5 | 2356 | 4053.46 |
| volume | 94640 | 94640 | 35840 | 35840 | 12039.44 | 4386.5235 |
| T | 516.65 | 517.73 | 517.77 | 518.36 | 500.9 | 514.282 |
| volume | 296240 | 181440 | 181440 | 94640 | 36260.12 | 516.63722 |
| S_w | 0.26 | 0.263 | 0.292 | 0.295 | 0.511 | 0.3242 |
| volume | 296240 | 296240 | 181440 | 181440 | 36260.12 | 0.2823336 |
| S_g | 0.745 | 0.737 | 0.741 | 0.738 | 0.465 | 0.6852 |
| volume | 94640 | 94640 | 35840 | 35840 | 12039.44 | 0.7284344 |

APPENDIX A.2: Graphical Results Obtained from Simulator for Steam Injection Rates and Steam Injection Quality Variations.

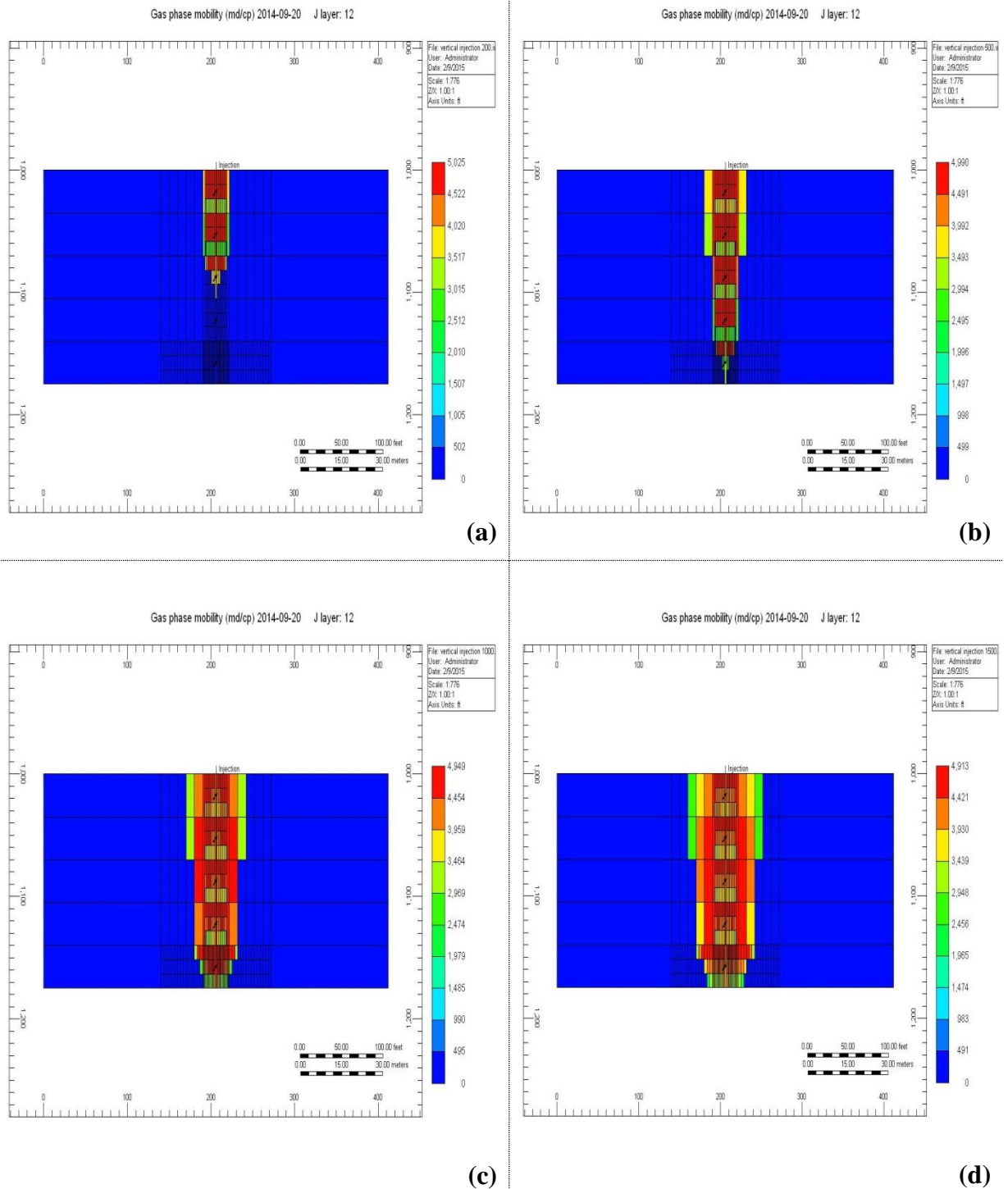
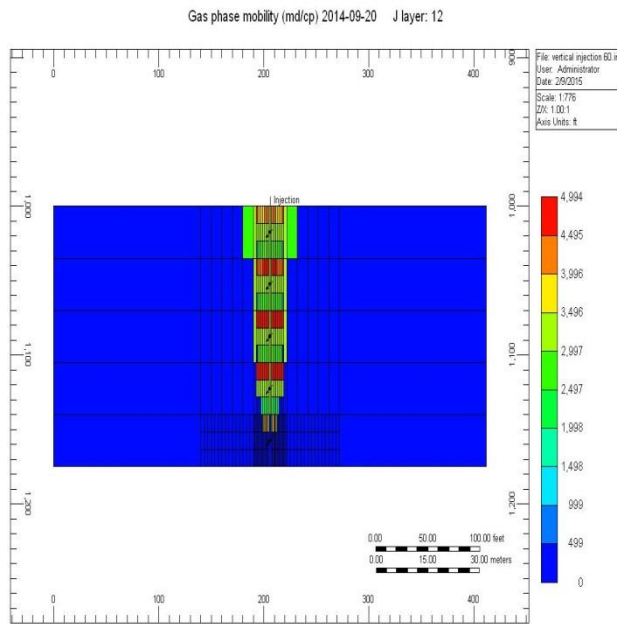
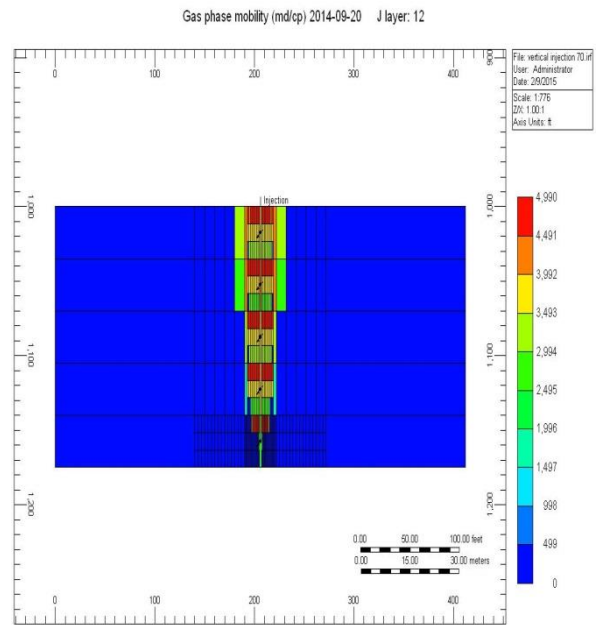


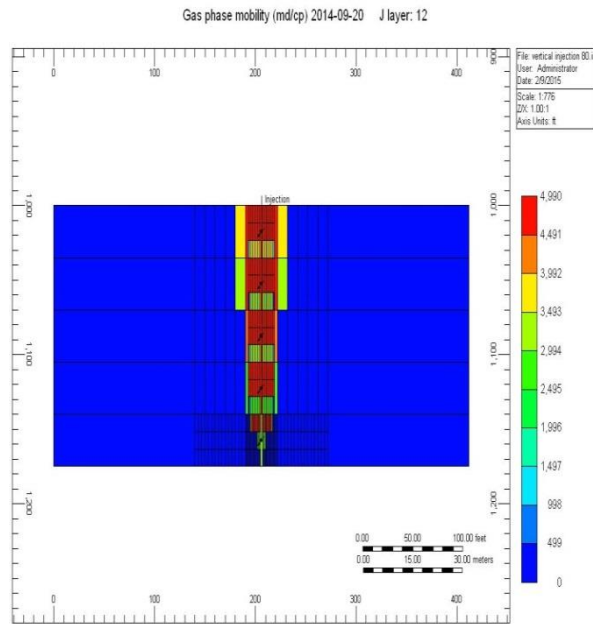
Figure A.1 : Steam injection rates: (a) 200 STB/day, (b) 500 STB/day, (c) 1000 STB/day, (d) 1500 STB/day.



(a)



(b)



(c)

Figure A.2 : Steam injection qualities: (a) 60%, (b) 70%, (c) 80%.



CURRICULUM VITAE

Name Surname: Elnaz Ghafouri Aian

Place and Date of Birth: Iran and 03.04.1985

E-Mail: elnaz.ghafuri@gmail.com

EDUCATION:

B.Sc.: Chemical Engineering

M.Sc.: Petroleum and Natural Gas Engineering

PROFESSIONAL EXPERIENCE AND REWARDS:

PUBLICATIONS, PRESENTATIONS AND PATENTS ON THE THESIS:

- Ghafouri, E.A., Türeyn. Ö.İ., Satman, A., 2015. IPETGAZ, *International Petroleum and Natural Gas Congress and Exhibition of Turkey*, May 27-29, Ankara, Turkey.